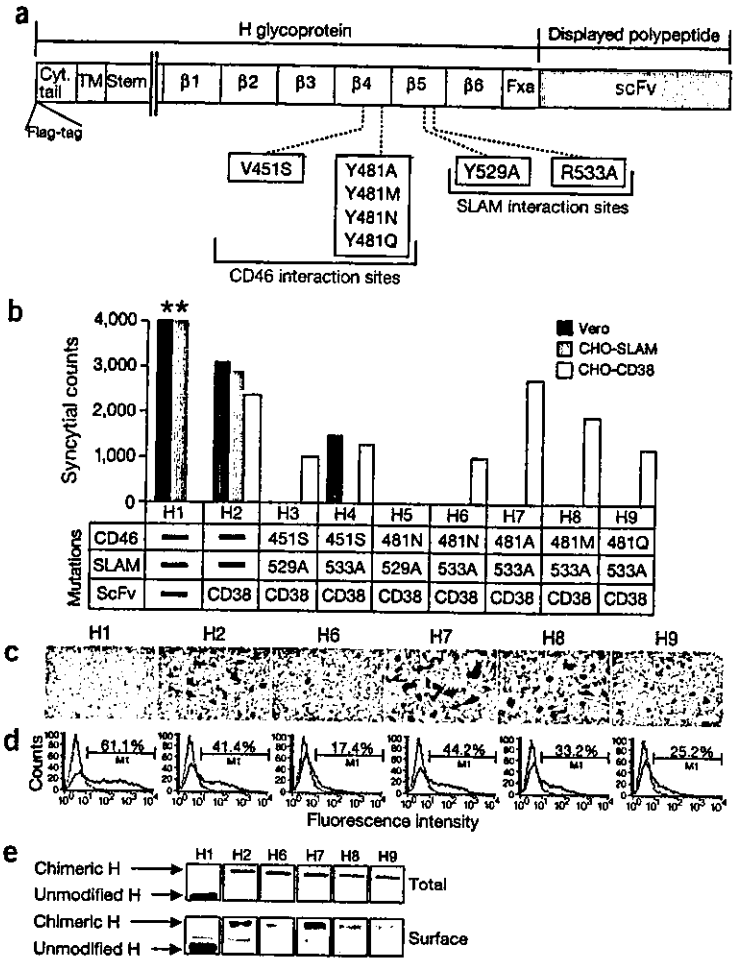

Figure 1 Fusogenic properties of mutant H glycoproteins displaying anti-CD38 antibody. (a) Schematic representation of MV-Edm H protein[37] showing H residues mediating CD46 or SLAM interactions. The single-chain antibody is displayed as a C-terminal extension of H glycoprotein and an N-terminal FLAG tag (DYKDDDK) is included to facilitate immunoblot detection. cyt., cytoplasmic; TM, transmembrane; Fxa, Factor Xa cleavage site (IEGR). Standard one-letter abbreviations are used to denote amino acid residues. (b) Receptor-specific fusion support by chimeric H expression plasmids after cotransfection with measles F plasmid. Syncytia in five representative fields were counted, and the number of syncytia per well was calculated. Asterisks indicate that the syncytia were not countable because >90% of the cells were in syncytia. (c) CHO-CD38 cells were cotransfected with indicated H expression plasmids and measles F, and syncytia were photographed 24 h later. Scale bar, 200 μm. (d) Cell surface expression of chimeric H proteins (bold lines), relative to mock transfected cells (thin lines) was determined by FACS analysis after labeling with anti-H antibody. See b for H-construct designations. (e) Total and cell surface H protein expression levels were also estimated by immunoblotting of cell lysates or of surface biotinylated proteins immunoprecipitated with anti-Flag antibody. See b for H-construct designations. The fusogenic activities of the CD38-displaying H chimeras correlate closely with their levels of surface expression.

different chimeric H protein expression plasmids was similar (Fig. 1e). However, cell surface expression, determined by immunoprecipitation of surface biotinylated protein (Fig. 1e) and by fluorescence-activated cell sorting (FACS) analysis (Fig. 1d), differed substantially among the various chimeras. Cell surface expression of every chimeric H protein tested was consistently in accord with the intensity of its fusion support activity on CHO-CD38 cells. In particular, the slightly higher surface expression of the doubly ablated H_{AA}-CD38 mutant in comparison to the nonablated H-CD38 chimera showed that the Y481A and R533A mutations provide the optimal platform for generation of fully retargeted H proteins by scFv display. Indeed, this conclusion was further confirmed by comparing panels of chimeric H proteins displaying alternative scFvs (data not shown).

To determine whether our findings could be generalized to scFvs targeting human cellular receptors other than CD38, we generated doubly ablated (Y481A, R533A) H-protein chimeras displaying C-terminal scFvs recognizing H_{AA}-CEA[16,22] or H_{AA}-EGFR[23]. Each of the doubly ablated, scFv-displaying chimeric H proteins supported fusion, leading to cell death exclusively in cells expressing the relevant targeted receptor (Fig. 2a,b). Background fusion via CD46 or SLAM was not observed. In contrast to these targeted H proteins, the unmodified H protein led to extensive syncytium formation and cytotoxicity in CHO-CD46 and CHO-SLAM cells. Thus, F protein–mediated cell fusion could be fully and accurately redirected through different antibody-receptor interactions by displaying scFvs at the C terminus of a doubly ablated, receptor-blind H protein.

Genes coding for fusogenic membrane glycoproteins have recently been exploited for cytoreductive gene therapy for cancer, whereby transduced cancer cells fuse with neighboring nontransduced cells, leading to tumor regression[9]. To demonstrate the potential of targeted cell fusion for cytoreductive gene therapy of human cancer, we generated bicistronic adenovirus vectors expressing measles F protein with EGFR-targeted, CD38-targeted or untargeted H proteins, and compared their specificity and potency against human ovarian SKOV3ip.1 tumor cells as a treatment model. SKOV3ip.1 cells express low levels of primary coxsackievirus-adenovirus receptor (CAR) and are therefore relatively resistant to adenovirus transduction (Fig. 3a). Adenoviral vectors were therefore used at relatively high multiplicity of infection, standardized to particle counts for all three vectors, to ensure a reasonable efficiency of transduction of ~1% of the tumor cells (Fig. 3b, first panel). The SKOV3ip.1 cells express abundant CD46 and abundant EGFR, but minimal CD38 (Fig. 3a). Surprisingly, in contrast to adenoviruses expressing untargeted measles H protein, the EGFR-targeted adenoviruses could mediate very efficient targeted fusion and killing of SKOV3ip.1 cells. One possible explanation for this difference is that there is a higher absolute density of EGFR compared with CD46 on the SKOV3ip.1 cells. Alternatively, it is possible that the efficiency of F protein triggering by receptor-bound H protein is intrinsically higher

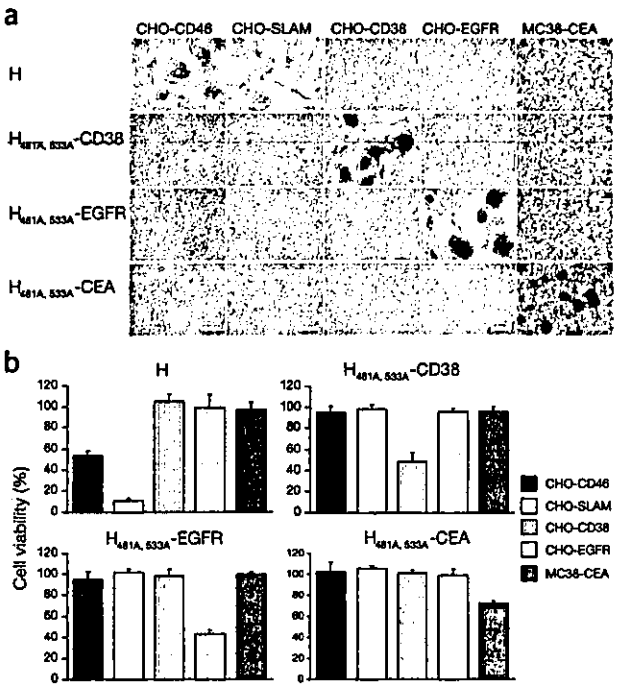

Figure 2 Antibody-targeted cell fusion and cell killing. (a) Target cells expressing indicated receptors were cotransfected with indicated H-expression plasmids plus measles F protein, and syncytia were photographed 24 h later. Scale bar, 200 μm. (b) Cell viability was determined 36 h after transfection and is shown as the percentage cell survival compared to control mock-transfected cultures. H proteins carrying Y481A and R533A mutations, and displaying cell-targeting scFvs to CD38, EGFR or CEA caused no fusion through CD46 or SLAM receptors, but efficiently mediated targeted cell fusion via CD38, EGFR or CEA, respectively.

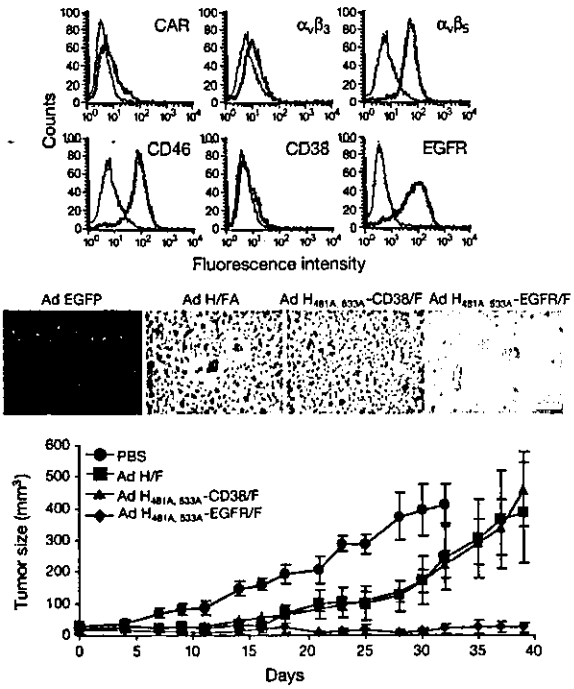

Figure 3 Targeted cytoreductive gene therapy using homologous targeted cell fusion. (a) Expression of relevant receptors by human SKOV3ip.1 ovarian tumor cells was determined by FACS analysis. (b) Cells were infected with adenoviral vectors expressing EGFP, measles F and H proteins, F protein with CD38-targeted H or F proteins with EGFR-targeted H protein at an MOI of 300 particles/cell. Cells were photographed 48 h after infection. Transduction with adenovirus vectors encoding EGFP is low due to deficiency of CAR. Transduction with the H/F vector led to moderate H/F-induced cell fusion. In contrast, the EGFR-targeted H/F vector caused massive cell fusion and cytotoxicity, whereas the CD38-targeted H/F vector had no effect on these CD38-negative SKOV3ip.1 cells. Scale bar, 200 μm. (c) Intratumoral injection of the EGFR-targeted H/F vector elicited potent antitumor effects in contrast to PBS, untargeted H/F and CD38-targeted H/F vectors, and three of six mice in the group showed complete regression.

after binding to EGFR. As expected, control vectors expressing the CD38-targeted H protein showed no fusion activity in SKOV3ip.1 cells.

We next evaluated the *in vivo* effects of these adenoviral vectors against well-established SKOV3ip.1 xenografts implanted subcutaneously in athymic mice. Adenoviral vectors mediating EGFR-targeted fusion showed much greater therapeutic potency in this intratumoral therapy model than control vectors mediating fusion through CD46 (untargeted) or CD38 ($P = 0.0013$ compared to PBS, or $P \leq 0.05$ compared to Ad H/F and Ad $H_{481A, 533A}$-CD38/F; comparisons made on day 32) (Fig. 3c). Histological analysis of explanted tumors 3 d after they were injected with the different adenoviral vectors showed that cell fusion was considerably more prominent in tumors inoculated with vector expressing the EGFR-targeted H protein (data not shown). Taken together, these data demonstrate the superior specificity and potency of vectors mediating antibody-targeted cell fusion in a clinically relevant, cytoreductive, gene therapy model.

Increasingly, cells are exploited as therapeutic agents and antibody-targeted fusion has considerable potential to enhance the therapeutic outcome; stem cells are used for tissue repair, immune effector cells for tumor therapy and vector-modified cells for delivery of diverse genetic payloads[2,24,25]. Recent evidence indicates that stem cell plasticity may be a direct consequence of cell fusion[25] and might therefore be greatly enhanced by directing the stem cells to fuse efficiently with a desired target tissue. Also, heterokaryons obtained by fusing tumor cells with professional antigen-presenting cells (APCs) are known to be potent stimulators of antitumor immunity[11,12]. Antibody-targeted fusion could be used to generate these hybrid cells *in situ* by directing APCs to fuse specifically with tumor cells. Finally, targeted cell fusion provides an appealing strategy to mediate the irreversible trapping of cellular gene delivery vehicles at predetermined target sites.

To demonstrate that heterologous cell fusion between an immune effector cell and an epithelial tumor could be accurately targeted, we infected K562 human erythroleukemic cells with adenoviral vectors expressing nontargeted, EGFR-targeted or CD38-targeted H proteins. K562 cells transduced with the EGFR-targeted or CD38-targeted vector did not fuse with each other but underwent heterologous fusion with EGFR-positive epithelial tumor cells (A431) or with CD38-expressing suspension Jurkat T cells, respectively (Fig. 4a,b). In addition, the EGFR-targeted heterologous fusion was blocked by the presence of anti-EGFR antibody whereas the nontargeted heterologous fusion between K562 and A431 was not (Fig. 4c). An important question arising from these studies relates to the stability of the hybrid cells generated by this method. This is currently under investigation as it is likely to be a key parameter for some of the suggested applications. Our preliminary observation is that the stability of the cell hybrids

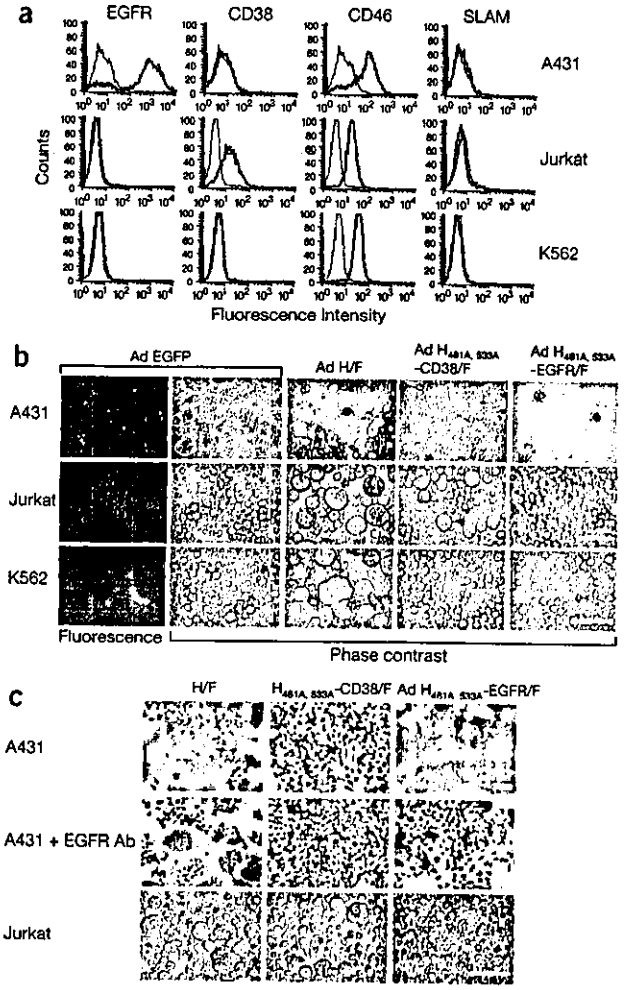

Figure 4 Adenoviral vectors mediating homologous or heterologous targeted cell fusion. (a) Expression of relevant receptors by human tumor cell lines was determined by FACS analysis. (b) Cell lines were infected with adenoviral vectors expressing EGFP, measles F and H proteins, F with CD38-targeted H or F proteins with EGFR-targeted H protein at an MOI of 1,000 particles/cell (for A431) or 10,000 particles/cell (for Jurkat T and K562 cells). Cells were photographed 48 h after infection. Adenovirus vectors encoding CD38 and EGFR-targeted H proteins could mediate targeted fusion and killing of CD38-positive Jurkat T cells or EGFR-positive A431 cells, respectively, but not of receptor-negative K562 cells. The red arrow indicates a syncytium and the white arrow indicates a single cell. (c) However, washed K562 cells expressing CD38 or EGFR-targeted H proteins readily underwent heterologous antibody-targeted cell fusion within 12 h when added to CD38-positive Jurkat T or EGFR-positive A431 cells, respectively. In addition, heterologous EGFR-targeted fusion of adenovirus-infected K562 cells was selectively blocked in the presence of anti-EGFR 528 antibody (EGFR Ab; final concentration 200 ng/ml). Scale bar, 80 μm (b,c).

varies greatly depending upon cell lineage, culture conditions and the number of cell nuclei in each syncytium.

The three cellular receptors targeted in this study belong to widely differing receptor families. CD38 is a 45 kDa type II transmembrane glycoprotein with NAD(P)$^+$glycohydrolase and cell signaling activity[26]; CEA is a heavily glycosylated type I membrane glycoprotein involved in cell adhesion[27]; and EGFR is a type I membrane glycoprotein that undergoes dimerization and rapid endocytosis upon binding EGF[28]. Thus, our data suggest that receptor choice is not a limitation for cell fusion and that it should be possible to target the process through a broad array of cell surface antigens, irrespective of their particular structure. Besides giving insight into the remarkable plasticity of cell fusion triggering mechanisms, antibody-targeted fusion has great potential as a research tool and provides a versatile platform for novel targeted therapies.

METHODS

Cell culture. Vero African green monkey kidney cells (#CCL-81), A431 human epidermoid carcinoma cells (#CRL-1555), Jurkat T-cell leukemia cells (#TIB-152) and K562 human erythroleukemic cells (#CCL-243) were purchased from American Type Culture Collection (ATCC). All cell lines were grown at 37 °C in media recommended by the suppliers in a humidified atmosphere of 5% CO_2. The SKOV3ip.1 ovarian tumor cells were maintained in alpha-MEM (Irvine Scientific) supplemented with 20% (v/v) FBS (Gibco). CHO-CD46 cells were generated by stable transfection of the parental CHO cells using a CD46-C1 isoform expression plasmid[29]. CHO clones stably expressing CD46 were selected using 1.2 mg/ml G418 (Gibco-BRL). Clones expressing high levels of CD46 were identified by flow cytometry using a fluorescein isothiocyanate (FITC)-conjugated, anti-CD46 antibody (Pharmingen). The CHO-CD46 and CHO-CD38[17] cells were grown and maintained in DMEM (Gibco) containing 10% (v/v) FBS, penicillin and streptomycin (DMEM-10) at 37 °C in an atmosphere of 5% CO_2 with 1 mg of G418/ml. CHO-EGFR cells[30] and MC38-cells[31] were grown and maintained in DMEM-10 with 0.5 mg/ml of G418 at 37 °C in an atmosphere of 5% CO_2. CHO-SLAM cells[14] were grown in RPMI 1640 (Gibco) containing 10% FBS, penicillin and streptomycin with 0.5 mg/ml of G418 at 37 °C in an atmosphere of 5% CO_2.

H expression plasmids, transfections and cell fusion assay. Site-directed mutagenesis of pCGHX α-CD38, a measles H glycoprotein expression construct displaying the CD38 scFv[17], was done using the Quick-Change system (Stratagene). Constructs encoding chimeric H proteins with C-terminal scFvs recognizing CEA[22] or EGFR[23] were easily made by exchanging the CD38 scFv fragment via flanking *Sfi*I and *Not*I cloning sites. Cells (8×10^4/well in 24-well plates) were cotransfected with 0.5 μg pCGF, a measles F expression plasmid[32] and 0.5 μg of the appropriate H mutant expression plasmid using Superfect (Qiagen). At 24 h after transfection, the cells were fixed in 0.5% (v/v) glutaraldehyde and stained with 0.1% (w/v) crystal violet, and the syncytia were scored and photographed. For cytotoxicity studies, cells (2×10^4/well in 96-well plates) were transfected with 0.25 μg of pCGF plasmid and 0.25 μg of the appropriate H-protein plasmid, and cell viability was assessed 36 h after transfection using the CellTiter96R Aqueous Non-Radioactive Cell Proliferation Assay (Promega). Results represent means ± s.d. of triplicate determinations.

Surface biotinylation, western blotting and FACS analysis. Cells (4×10^5/well in 6-well plates) were transfected with the appropriate H-protein mutant expression plasmids. After 24 h, the transfected cells were washed two times with 1 ml of ice-cold PBS, and surface proteins were labeled with biotin-7-*N*-hydroxysuccinimide ester for 15 min at 20 °C using a Cellular Labeling kit (Roche). The reaction was stopped by adding NH_4Cl (final concentration, 50 mM) for 15 min at 4 °C. The cells were then washed once, and treated with 500 μl of lysis buffer (50 mM Tris, pH 7.5, 1% (v/v) Igepal CA-630 (Sigma), 1 mM EDTA, 150 mM NaCl, protease inhibitor cocktail (Sigma)) for 15 min at 4 °C, and the lysates were subjected to centrifugation at 4 °C for 15 min at 12,000*g*. Then 20 μl of the resulting postnuclear fraction was directly mixed with an equal volume of SDS loading buffer (130 mM Tris, pH 6.8, 20% (v/v) glycerol, 10% (v/v) SDS, 0.02% (w/v) bromophenol blue, 100 mM dithiothreitol). These samples (40 μl) were denatured for 5 min at 95 °C, fractionated on a 7.5% SDS-polyacrylamide gel, blotted to polyvinylidene difluoride membranes (Bio-Rad), immunoblotted with anti-Flag M2 antibody conjugated to horseradish peroxidase (Sigma) and developed using an enhanced chemiluminescence kit (Pierce) for detection of total H protein. The biotinylated H proteins were immunoprecipitated with anti-Flag antibodies using an immunoprecipitation kit (Roche). We mixed 50 μl of protein A–coated agarose beads with

350 µl of the postnuclear supernatant and 1 µl of anti-Flag M2 antibody (Sigma), followed by overnight incubation at 4 °C under rotation. The agarose beads were then washed three times before resuspension in 50 µl of loading buffer and boiled for 2 min at 100 °C to elute bound proteins. As described above, the samples (40 µl) were fractionated on an SDS-polyacrylamide gel, blotted to polyvinylidene difluoride membranes, and probed with peroxidase-coupled streptavidin (Roche), followed by detection of surface H protein using an enhanced chemiluminescence kit. Alternatively, the surface expression level of H protein was detected by FACS analysis. Twenty-four hours after transfection of the appropriate H mutant or mock plasmid, cells were washed twice with PBS and resuspended in ice-cold PBS containing 2% (v/v) FBS at a concentration of 10^5 cells/ml. The cells were then incubated for 60 min on ice with 1:150 final dilution of the primary mouse monoclonal ascites antibody recognizing measles H protein (Chemicon). Subsequently, the cells were washed with 2% (v/v) FBS/PBS and incubated for an additional 30 min with 1:150 final dilution of FITC-conjugated goat anti-mouse IgG (Santa Cruz Biotechnology). After washing with 2% (v/v) FBS/PBS, the cells were analyzed by flow cytometry using a FACScan system with CELLQuest software (Becton Dickinson). Expression of relevant receptors in A431, Jurkat T cells and K562 human tumor cells was similarly detected by FACS analysis using anti-EGFR 528 (Santa Cruz Biotechnology), anti-CD38, anti-CD46, anti-SLAM antibodies (Pharmingen), anti-CAR antibody RmcB (ATCC), anti-$\alpha_v\beta_3$ antibody (Chemicon) or anti-$\alpha_v\beta_5$ antibody (Gibco).

Adenoviral vectors. All recombinant adenoviruses were constructed using an *in vitro* ligation method as described previously[33]. H, H_{AA}-CD38, H_{AA}-EGFR or EGFP (Clontech) coding sequences were cloned downstream of a human cytomegalovirus immediate early promoter/enhancer ($P_{CMV\ IE}$) in the pHM5 shuttle vector. The F gene was cloned downstream of the $P_{CMV\ IE}$ in the pHM11 shuttle vector. Expression cassettes were transferred from the pHM5 or pHM11 shuttle vectors into the E1 or E3-deleted regions, respectively, of the adenoviral vector plasmid pAdHM48. Genes encoding H protein and EGFP were cloned into the E1 site and the gene encoding F was cloned into E3. The resulting recombinant adenovirus genomes were transfected into human embryonic kidney (HEK)-293 cells. Because expression of measles F and H proteins causes cell fusion and is toxic to HEK-293 cells, viruses were rescued in the presence of a fusion inhibitory peptide (FIP; Bachem), which blocks F/H-protein mediated fusion[34]. The resulting recombinant adenoviruses were propagated in HEK-293 cells in the presence of FIP peptide, and were purified by CsCl-equilibrium centrifugation as described previously[35]. Purified virion preparations were dialyzed against 10 mM PBS, 10% (v/v) glycerol, and finally stored at −80 °C. Viral particle numbers (particles/ml) were calculated from optical density measurements at 260 nm (OD_{260})[36]. All viruses showed similar physical particle titers of approximately 10^{11} particles/ml: Ad EGFP, 1.41×10^{11}; d H/F, 5.75×10^{11}; Ad $H_{481A,533A}$-CD38/F, 2.59×10^{11}; Ad $H_{481A,533A}$-EGFR/F, 3.20×10^{11}.

In vivo experiments. All experimental protocols are approved by the Mayo Foundation Institutional Review Board and Institutional Animal Care and Use Committee. To establish subcutaneous tumors, 6-week-old athymic nu/nu female mice (Harlan Sprague Dawley) were injected with 5×10^6 tumor cells. When the tumors measured 0.3–0.4 cm in diameter, mice received four intratumoral injections of Ad H/F ($n = 6$), Ad $H_{481A,533A}$-CD38/F ($n = 5$), or Ad $H_{481A,533A}$-EGFR/F ($n = 6$) at 7×10^9 viral particles (total 2.8×10^{10}), on days 0, 1, 3 and 4. Control tumors were injected with an equal volume of PBS only ($n = 5$). Animals were killed at the end of the experiment, when tumor burden reached 10% of body weight or when ulcer was seen in tumor. The tumor diameter was measured three times per week and the volume (product of 0.5 × length × length × width) was calculated as mean ± s.e.m. Statistical analysis was performed by analysis of variance followed by Fisher's test, and $P < 0.05$ was considered to be statistically significant.

ACKNOWLEDGMENTS

We thank C.D. James for CHO-EGFR cells, Y. Yanagi for CHO-SLAM cells, J. Schlom for MC38-CEA cells, E. Vitetta for SKOV3ip.1 cells, J.P. Atkinson for CD46 plasmid, J.A. Lust for CD38 scFv, R. Hawkins for CEA scFv and G. Winter for EGFR scFv. We also thank M.J. Federspiel and R.G. Vile for critical reading of the manuscript. This study is supported by the Mayo Foundation, Harold W. Siebens Foundation and NIH grants CA100634-01 and CA90636-01.

COMPETING INTERESTS STATEMENT

The authors declare that they have no competing financial interests.

Received 17 October; accepted 11 December 2003
Published online at http://www.nature.com/naturebiotechnology/

1. Shemer, G. & Podbilewicz, B. Fusomorphogenesis: cell fusion in organ formation. *Dev. Dyn.* **218**, 30–51 (2000).
2. Holden, C. & Vogel, G. Stem cells. Plasticity: time for a reappraisal. *Science* **296**, 2126–2129 (2002).
3. Griffin, D.E. Measles Virus. in *Fields Virology* (eds. Knipe, D.M. & Howley, P.M.) 1402–1442 (Lippincott Williams & Wilkins, Philadelphia, 2001).
4. Freed, E.O. & Martin, M.A. HIVs and their replication. in *Fields Virology* (eds. Knipe, D.M. & Howley, P.M.) 1971–2042 (Lippincott Williams & Wilkins, Philadelphia, 2001).
5. Cohen, J.I. & Straus, S.E. Varicella-Zoster virus and its replication. in *Fields Virology* (eds. Knipe, D.M. & Howley, P.M.) 2707–2730 (Lippincott Williams & Wilkins, Philadelphia, 2001).
6. Kohler, G. & Milstein, C. Continuous cultures of fused cells secreting antibody of predefined specificity. *Nature* **256**, 495–497 (1975).
7. Dorssers, L.C. & Veldscholte, J. Identification of a novel breast-cancer-anti-estrogen-resistance (BCAR2) locus by cell-fusion-mediated gene transfer in human breast-cancer cells. *Int. J. Cancer* **72**, 700–7005 (1997).
8. Dieken, E.S., Epner, E.M., Fiering, S., Fournier, R.E. & Groudine, M. Efficient modification of human chromosomal alleles using recombination-proficient chicken/human microcell hybrids. *Nat. Genet.* **12**, 174–182 (1996).
9. Galanis, E. *et al.* Use of viral fusogenic membrane glycoproteins as novel therapeutic transgenes in gliomas. *Hum. Gene Ther.* **12**, 811–821 (2001).
10. Peng, K.W. *et al.* Intraperitoneal therapy of ovarian cancer using an engineered measles virus. *Cancer Res.* **62**, 4656–4662 (2002).
11. Guo, Y. *et al.* Effective tumor vaccine generated by fusion of hepatoma cells with activated B cells. *Science* **263**, 518–520 (1994).
12. Bateman, A. *et al.* Fusogenic membrane glycoproteins as a novel class of genes for the local and immune-mediated control of tumor growth. *Cancer Res.* **60**, 1492–1497 (2000).
13. Dorig, R.E., Marcil, A., Chopra, A. & Richardson, C.D. The human CD46 molecule is a receptor for measles virus (Edmonston strain). *Cell* **75**, 295–305 (1993).
14. Tatsuo, H., Ono, N., Tanaka, K. & Yanagi, Y. SLAM (CDw150) is a cellular receptor for measles virus. *Nature* **406**, 893–897 (2000).
15. von Messling, V., Zimmer, G., Herrler, G., Haas, L. & Cattaneo, R. The hemagglutinin of canine distemper virus determines tropism and cytopathogenicity. *J. Virol.* **75**, 6418–6427 (2001).
16. Hammond, A.L. *et al.* Single-chain antibody displayed on a recombinant measles virus confers entry through the tumor-associated carcinoembryonic antigen. *J. Virol.* **75**, 2087–2097 (2001).
17. Peng, K.W. *et al.* Oncolytic measles viruses displaying a single-chain antibody against CD38, a myeloma cell marker. *Blood* **101**, 2557–2562 (2003).
18. Lecouturier, V. *et al.* Identification of two amino acids in the hemagglutinin glycoprotein of measles virus (MV) that govern hemadsorption, HeLa cell fusion, and CD46 downregulation: phenotypic markers that differentiate vaccine and wild-type MV strains. *J. Virol.* **70**, 4200–4204 (1996).
19. Vongpunsawad, S., Oezgum, N., Braun, W. & Cattaneo, R. Selectively receptor-bind measles viruses: Identification of the SLAM-and CD46-interacting residues and their localization on a new hemagglutinin structural model. *J. Virol.* **78**, 302–313 (2004).
20. Xie, M., Tanaka, K., Ono, N., Minagawa, H. & Yanagi, Y. Amino acid substitutions at position 481 differently affect the ability of the measles virus hemagglutinin to induce cell fusion in monkey and marmoset cells co-expressing the fusion protein. *Arch. Virol.* **144**, 1689–1699 (1999).
21. Cattaneo, R. & Rose, J.K. Cell fusion by the envelope glycoproteins of persistent measles viruses which caused lethal human brain disease. *J. Virol.* **67**, 1493–1502 (1993).
22. Chester K.A. *et al.* Phage libraries for generation of clinically useful antibodies. *Lancet* **343**, 455–456 (1994).
23. Kettleborough, C.A., Saldanha, J., Heath, V.J., Morrison, C.J. & Bendig, M.M. Humanization of a mouse monoclonal antibody by CDR-grafting: the importance of framework residues on loop conformation. *Protein Eng.* **4**, 773–783 (1991).
24. Wang, G. *et al.* A T cell-independent antitumor response in mice with bone marrow cells retrovirally transduced with an antibody/Fc-gamma chain chimeric receptor gene recognizing a human ovarian cancer antigen. *Nat. Med.* **4**, 168–172 (1998).
25. Wang, X. *et al.* Cell fusion is the principal source of bone-marrow-derived hepatocytes. *Nature* **422**, 897–901 (2003).
26. Mehta, K., Shahid, U. & Malavasi, F. Human CD38, a cell-surface protein with multiple functions. *FASEB J.* **10**, 1408–1417 (1996).
27. Obrink, B. CEA adhesion molecules: multifunctional proteins with signal-regulatory properties. *Curr. Opin. Cell Biol.* **9**, 616–626 (1997).
28. Carpenter, G. Receptor tyrosine kinase substrates: src homology domains and signal transduction. *FASEB J.* **6**, 3283–3289 (1992).
29. Kemper, C. *et al.* Activation of human $CD4^+$ cells with CD3 and CD46 induces a T-regulatory cell 1 phenotype. *Nature* **421**, 388–392 (2003).
30. Schneider, U., Bullough, F., Vongpunsawad, S., Russell, S.J. & Cattaneo, R.

Recombinant measles viruses efficiently entering cells through targeted receptors. *J. Virol.* **74**, 9928–9936 (2000).
31. Robbins, P.F. *et al.* Transduction and expression of the human carcinoembryonic antigen gene in a murine colon carcinoma cell line. *Cancer Res.* **51**, 3657–3662 (1991).
32. Cathomen, T., Buchholz, C.J., Spielhofer, P. & Cattaneo, R. Preferential initiation at the second AUG of the measles virus F mRNA: a role for the long untranslated region. *Virology* **214**, 628–632 (1995).
33. Mizuguchi, H., Xu, Z.L., Sakurai, F., Mayumi, T. & Hayakawa, T. Tight positive regulation of transgene expression by a single adenovirus vector containing the rtTA and tTS expression cassettes in separate genome regions. *Hum. Gene Ther.* **14**, 1265–1277 (2003).
34. Firsching, R. *et al.* Measles virus spread by cell-cell contacts: uncoupling of contact-mediated receptor (CD46) downregulation from virus uptake. *J Virol.* **73**, 5265–5273 (1999).
35. Kanegae, Y. *et al.* Efficient gene activation in mammalian cells by using recombinant adenovirus expressing site-specific Cre recombinase. *Nucl. Acids Res.* **23**, 3816–3821 (1995).
36. Mittereder, N., March, K.L. & Trapnell, B.C. Evaluation of the concentration and bioactivity of adenovirus vectors for gene therapy. *J. Virol.* **70**, 7498–7509 (1996).
37. Langedijk, J.P., Daus, F.J., & van Oirschot, J.T. Sequence and structure alignment of Paramyxoviridae attachment proteins and discovery of enzymatic activity for a morbillivirus hemagglutinin. *J. Virol.* **71**, 6155–6167 (1997).

[CANCER RESEARCH 63, 4420–4425, August 1, 2003]

Antitumor Effect by Interleukin-11 Receptor α-Locus Chemokine/CCL27, Introduced into Tumor Cells through a Recombinant Adenovirus Vector[1]

Jian-Qing Gao, Yasuhiro Tsuda, Kazufumi Katayama, Takashi Nakayama, Yutaka Hatanaka, Yoichi Tani, Hiroyuki Mizuguchi, Takao Hayakawa, Osamu Yoshie, Yasuo Tsutsumi, Tadanori Mayumi, and Shinsaku Nakagawa[2]

Department of Biopharmaceutics, Graduate School of Pharmaceutical Sciences, Osaka University, Suita, Osaka 565-0871 [J-Q. G., Y. Tsud., K. K., Y. Tsut., T. M., S. N.]; Department of Microbiology, Kinki University School of Medicine, Osaka-Sayama, Osaka 589-8511 [T. N., O. Y.]; Department of Biomedical Science, DakoCytomation Company Ltd., Nishinotoin-higashiiru, Shijo-dori, Shimogyo, Kyoto 600-8493 [Y. H., Y. Ta.]; and Division of Cellular and Gene Therapy Products, National Institute of Health Sciences, Setagaya-ku, Tokyo 158-8501 [H. M., T. H.], Japan

ABSTRACT

In this study, we examined antitumor activity of a mouse CC chemokine ILC/CCL27 and a mouse CX_3C chemokine fractalkine/CX_3CL1 *in vivo*. We generated recombinant adenovirus vectors with a fiber mutation, encoding mILC (Ad-RGD-mILC) and mFKN (Ad-RGD-mFKN). We confirmed tumor cells infected with Ad-RGD-mILC and Ad-RGD-mFKN to express and release these chemokines. Tumor rejection experiments *in vivo* were carried out by inoculating OV-HM cells infected with Ad-RGD-mILC or Ad-RGD-mFKN into immunocompetent mice. mILC significantly suppressed the tumor growth, whereas no such significant effect was observed by mFKN. The antitumor activity induced by mILC was T cell dependent, involving both $CD4^+$ and $CD8^+$ T cells. Immunohistochemical analysis revealed accumulation of both $CD3^+$ lymphocytes and NK cells in the tumor tissue transduced with mILC and mFKN. However, there was a significant difference in the distribution of infiltrating cells. Furthermore, mFKN appeared to have an angiogenic activity, which might have masked its tumor suppressive activity. Collectively, ILC/CCL27 may be a good candidate molecule for cancer gene therapy.

INTRODUCTION

Considerable attention has been paid recently to the application of chemokines to cancer immunotherapy, because of their chemotactic activity for a variety of immune cells, as well as angiostatic activity of some chemokines, such as IFN-inducible protein-10/CXCL10 and Mig/CXCL9. In addition, it has been known that some tumor cells express a lower level of chemokines than that of normal cells (1). The tumor suppressive activity of several chemokines was also observed after these genes had been transduced into a variety of experimental tumors (2–9). Tumor cells that were transduced with the CC chemokine, macrophage inflammatory protein-1α/CCL3, had reduced tumorgenicity and significantly increased infiltration of macrophage and neutrophil (7). A strong leukocyte-mediated inflammatory response was observed in tumors expressing macrophage inflammatory protein-1α, leading to the induction of strong antitumor CTL responses (8). Another CC chemokine, macrophage-derived chemokine/CCL22, also had a strong chemoattractant activity for dendritic, NK,[3] and T cells, resulting in tumor regression in a murine lung carcinoma model by its efficient induction of antitumor immunity (9).

More than 40 chemokines have thus far been well characterized (10), but only a few have been demonstrated as candidates for cancer therapy by using as sole agents or with adjuvant. In the present study, a CC family chemokine, ILC/CCL27, and a CX_3C chemokine, FKN/CX_3CL1, have been studied. ILC is expressed in the skin and selectively chemoattracts CLA^+ memory T and Langerhans cells (11, 12). FKN shows chemotactic activity for NK cells, T cells, and monocytes (13, 14). FKN is expressed by dendritic cells, and the expression is up-regulated on dendritic cell maturation (15). We hypothesized that if tumor cells could be genetically modified *in vitro* to produce chemokines *in vivo*, the chemokines would accumulate T cells in the tumor. The *in vivo* interaction of T cells with the tumor cells should induce antitumor immunity, resulting in suppression of tumor growth. To test this hypothesis, we used a recombinant adenovirus vector with a fiber mutation (Ad-RGD) containing the Arg-Gly-Asp (RGD) sequence in the fiber knob. This vector has been demonstrated to possess higher transduction and antitumor activities when we used it for cytokine gene therapy against melanoma, compared with conventional adenovirus vectors (16, 17). In this study, the ovarian carcinoma OV-HM cell line (18) was infected with a chemokine-encoding vector, Ad-RGD-mILC or Ad-RGD-mFKN, and inoculated into mice to test its antitumor activity in gene immunotherapy. Ad-RGD-mILC induced the local recruitment of immune cells and suppressed tumor growth. By contrast, Ad-RGD-mFKN did not have such significant antitumor activity against OV-HM cells, although the tumor cells also attracted infiltrating immune cells.

MATERIALS AND METHODS

Cell Lines and Animals. OV-HM ovarian carcinoma cells were kindly provided by Dr. Hiromi Fujiwara (School of Medicine, Osaka University, Japan) and maintained in RPMI 1640 supplemented with 10% heat-inactivated FBS. B16/BL6, A549 lung carcinoma, and human embryonic kidney 293 cells were cultured in DMEM supplemented with 10% FBS. L1.2-mCCR10 and L1.2-mCX_3CR1 cells were maintained in RPMI 1640 supplemented with 10% heat-inactivated FBS and 2-ME (50 μM; Life Technologies, Inc.). All of the cell lines were cultured at 37°C in a humidified atmosphere with 5% CO_2. Female B6C3F1 and BALB/c nude mice were purchased from SLC, Inc. (Hamamatsu, Japan) and used at 6–8 week of age. All of the experimental procedures were in accordance with the Osaka University guidelines for the welfare of animals in experimental neoplasia.

Adenovirus Vectors. Replication-deficient adenovirus vectors with a fiber mutation used in this study were based on the adenovirus serotype 5 backbone with deletions of E1 and E3 and the expression cassette in the E1 region (19). The RGD sequence was inserted into the HI loop of the fiber knob using a two-step method developed by Mizuguchi *et al.* (20). Murine chemokine genes derived from pFastBac1-mILC and pBlueScriptSK(+)-mFKN were used as sources of their cDNA. Recombinant adenovirus vectors with the RGD fiber mutation, Ad-RGD-mILC and Ad-RGD-mFKN carrying the chemokine cDNA under the control of the cytomegalovirus promoter, were constructed by an improved *in vitro* ligation method as described (19, 21). The Ad-RGD-NULL vector, serving as a negative control, is identical to the Ad-RGD-mILC and Ad-RGD-mFKN vectors without the chemokine gene in the expression cassette. The adenovirus vectors were propagated in human embryonic kidney 293 cells and purified by cesium chloride gradient ultracentrifugation, and their titer was determined by plaque-forming assay using 293 cells (22, 23).

Received 12/4/02; accepted 5/23/03.

The costs of publication of this article were defrayed in part by the payment of page charges. This article must therefore be hereby marked *advertisement* in accordance with 18 U.S.C. Section 1734 solely to indicate this fact.

[1] This study was supported by grants from the Ministry of Health and Welfare in Japan and Grants-in-Aid for Scientific Research (C).

[2] To whom requests for reprints should be addressed, at Department of Biopharmaceutics, Graduate School of Pharmaceutical Sciences, Osaka University, Suita, Osaka 565-0871, Japan.

[3] The abbreviations used are: NK, natural killer; ILC, interleukin-11 receptor α-locus chemokine; FKN, fractalkine; RT-PCR, reverse transcription-PCR; FBS, fetal bovine serum; MOI, multiplicity of infection.

RT-PCR for Chemokine Gene Detection. To examine the expression of mILC and mFKN mRNA, OV-HM cells were infected with Ad-RGD-mILC, Ad-RGD-mFKN, or Ad-RGD-NULL, as a control vector, at an MOI of 10 for 24 h. After the 24-h cultivation, total RNA of the cells was isolated using TRIzol reagents (Life Technologies, Inc.). SuperScript II reverse transcriptase (Life Technologies, Inc.) was used for the cDNA reverse transcription. cDNA was amplified by PCR in the presence of primers (Pharmacia Biotechnology). Primer sequences for mILC were 5'-AGCAGCCTCCCGCTGTTACT-GTTG-3' (sense) and 5'-TGCTTTATTAGTTTTGCTGTTGGG-3' (antisense) and for mFKN were 5'-ATGACCTCACGAATCCCAGTGG-3'(sense) and 5'-CCGCCTCAAAACTTCCAATGC-3'(antisense). The following PCR conditions were used: (*a*) mILC: 30 s at 92°C, 60°C, and 72°C (30 cycles); and (*b*) mFKN: 30 s at 92°C, 55°C, and 72°C (30 cycles). PCR products were electrophoresed in 2% agarose gel and stained with ethidium bromide.

Chemotaxis Assay. A549 cells were infected at an MOI of 10 with Ad-RGD-mILC or Ad-RGD-mFKN for 24 h. The cells were washed and cultured for another 48 h. The resulting conditioned medium was collected, and its chemotactic activity was measured by migration assay across polycarbonate membrane (Chemotx 96; Neuro Probe; Ref. 24) using L1.2-mCCR10 or L1.2-mCX$_3$CR1 cells expressing the specific receptor for mILC or mFKN, respectively. Migration was allowed for 4 h at 37°C in a 5% CO_2 atmosphere. Migrated cells were lysed and quantitated by using a PicoGreen double-stranded DNA quantitation reagent (Molecular Probe).

Tumor Rejection in Mice and Subsequent Rechallenge by Tumor Reinoculation. Mice were inoculated intradermally into their flank with 1×10^6 OV-HM cells that had been infected with Ad-RGD-mILC or Ad-RGD-mFKN (at an MOI of 10 each in a volume of 100 μl diluted in RPMI 1640) for 24 h. Tumor volume was calculated by measuring the length and width of the tumor twice a week. Animals were euthanized when one of the two measurements was >15 mm. Three months after complete regression of primary tumors, mice were rechallenged with freshly isolated OV-HM tumor or B16/BL6 melanoma cells by intradermal injection of 1×10^6 cells into the flank. mILC gene-transduced OV-HM cells, made by transfection of Ad-RGD-mILC, were also inoculated into BALB/c nude mice to observe its antitumor activity.

T- or NK-cell Infiltration into OV-HM Tumors Expressing Chemokine. Immunohistochemical analysis was used to determine lymphocytes infiltrated into tumors. Tumor-bearing mice were sacrificed in 2 days after the administration of OV-HM cells transfected with Ad-RGD-mILC or Ad-RGD-mFKN. The tumor nodules were harvested, embedded in OCT compound (Sakura, Torrance, CA), and stored at −80°C. Frozen thin sections (6 μm in thickness) of the nodules were fixed in acetone, washed with PBS, and then incubated in PBS containing 0.3% hydrogen peroxide for 10 min at room temperature to block endogenous peroxidase activity. The sections were preincubated with 5% BSA in PBS for 10 min and sequentially incubated with optimal dilution of primary antibody, rabbit antiasialo GM1 (WAKO), rabbit antihuman CD3 antibody (DakoCytomation), or normal rabbit IgG (Santa Cruz Biotechnology). Each primary antibody bound was detected with biotinylated goat anti-rabbit immunoglobulins (DakoCytomation) and streptavidin-horseradish peroxidase (Vector Laboratories). Each of the incubations lasted for 30 min and was followed by a 15-min wash in Tris-buffered saline. The sections were stained with 3,3'-diaminobenzidine (WAKO) and finally counterstained with hematoxylin. The number of immunostained cells was counted under a light microscope with ×400 magnification.

Depletion of Lymphocytes and Tumor Growth. Injection (i.p.) of anti-mouse CD4 or CD8 ascitic fluid, 100 μl each, into mice was carried out seven times on days −3, −2, −1, 0, 5, 10, and 15. For NK cell depletion, mice were treated with asialo GM1 antiserum (40 μl/dose; WAKO) by i.p. injection six times on days −2, −1, 0, 5, 10, and 15. OV-HM cells infected with Ad-RGD-mILC at an MOI of 10 were intradermally inoculated on day 0. Tumor growth was examined twice a week.

RESULTS

Expression of mILC and mFKN by Infection with Adenovirus Vectors. We infected OV-HM, a mouse ovary carcinoma line, with recombinant adenovirus vectors encoding mILC or mFKN and examined their expression by RT-PCR at 24 h. As shown in Fig. 1, OV-HM cells infected with Ad-RGD-mILC and Ad-RGD-mFKN indeed expressed mILC and mFKN, respectively. To verify that mILC and mFKN produced by cells infected with the adenovirus vectors were biologically active, A549 cells were infected with the vectors for 24 h, and the culture supernatants were harvested after further cultivation for 48 h. The chemotactic activity in the culture supernatants was examined by a migration assay using L1.2-mCCR10 or L1.2-mCX$_3$CR1 cells. In this experiment, we used A549 cells instead of OV-HM cells because of a strong background chemotactic activity in the culture supernatant of the latter. As shown in Fig. 2, the culture supernatant of A549 cells infected with Ad-RGD-mILC and Ad-RGD-mFKN efficiently induced migration of L1.2-mCCR10 or L1.2-mCX$_3$CR1 cells, respectively. Because mFKN encoded by Ad-RGD-mFKN was the full-length transmembrane type, the results also suggested efficient generation of soluble mFKN through cleavage at the membrane-proximal site (13).

***In Vivo* Antitumor Effect by Infection with Ad-RGD-mILC.** OV-HM cells infected with Ad-RGD-mILC, Ad-RGD-mFKN, or Ad-RGD-NULL were intradermally inoculated into B6C3F1 mice. As shown in Fig. 3, OV-HM infected with Ad-RGD-mILC showed significant retardation in tumor growth *in vivo*. On the other hand, OV-HM infected with Ad-RGD-mFKN did not show any difference in tumor growth from that infected with Ad-RGD-NULL. In fact, 9 of 12 mice inoculated with OV-HM infected with Ad-RGD-mILC were tumor free (data not shown). In rechallenge experiment, mice that had complete regression were intradermally injected with OV-HM or B16/BL6 cells 90 days after the initial challenge. Results demonstrated that >50% of mice rechallenged with OV-HM (5 of 9 mice) remained tumor free for ≥2 months, whereas other mice showed

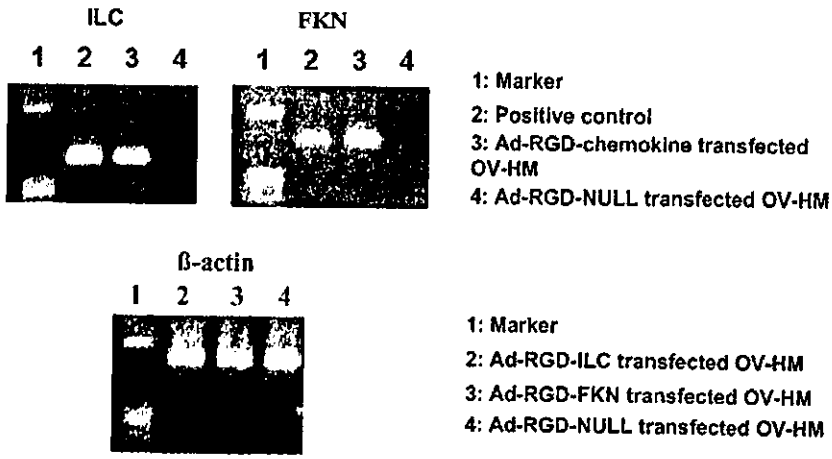

Fig. 1. RT-PCR analysis of chemokine mRNA expression in OV-HM cells infected with Ad-RGD-mILC or Ad-RGD-mFKN. Total RNA was isolated by TRIzol reagents from OV-HM cells infected with indicated chemokine-encoding adenovirus vectors at an MOI of 10 for 24 h, and SuperScript II reverse transcriptase was used for cDNA transcription. cDNA was amplified by PCR with indicated mouse chemokine-specific primers. Simultaneously, amplification of cDNA coding for β-actin was performed as an internal control. Amplified products were separated by 2% agarose gel electrophoresis and stained with ethidium bromide.

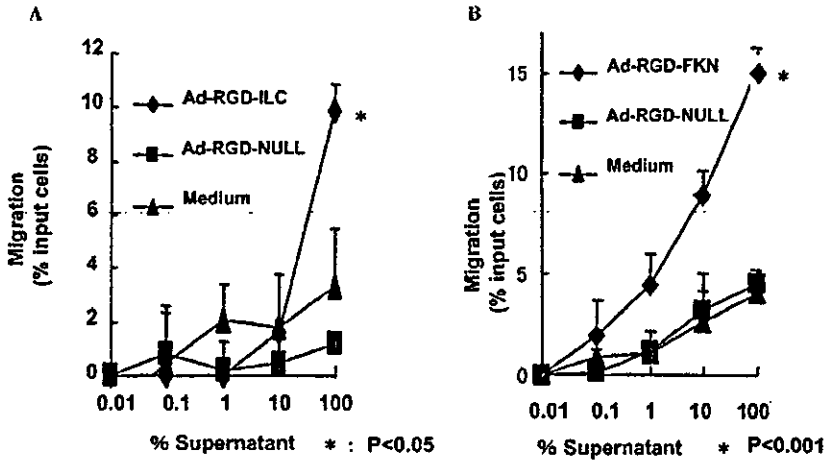

Fig. 2. Directed migration of cells, expressing chemokine receptors, induced by culture supernatants of A549 cells infected with Ad-RGD-ILC or Ad-RGD-FKN. A549 cells were infected at an MOI of 10 with: (*a*) Ad-RGD-mILC or (*b*) Ad-RGD-mFKN. After 24 h, the cells were washed and cultured for an additional 48 h. The culture supernatants were collected and used for the migration assay by adding to the bottom chamber. L1.2-mCCR10 or L1.2-mCX$_3$CR1 cells, expressing specific receptors for mILC or mFKN, respectively, were suspended at a concentration of 1×10^7cells/ml in migration buffer containing 1.04% RPMI 1640 without phenol red, 0.476% HEPES, and 0.5% BSA. After installing a filter on the bottom chamber, the cell suspensions, 20 μl each, were placed in the top chamber. Cell migration was allowed for 4 h at 37°C in a 5% CO_2 atmosphere. Migrated cells to the bottom chamber were lysed and quantitated by using a PicoGreen double-stranded DNA quantitation reagent. Data are expressed as the mean ± SD of triplicate results. Statistical analysis was carried out by Student's *t* test.

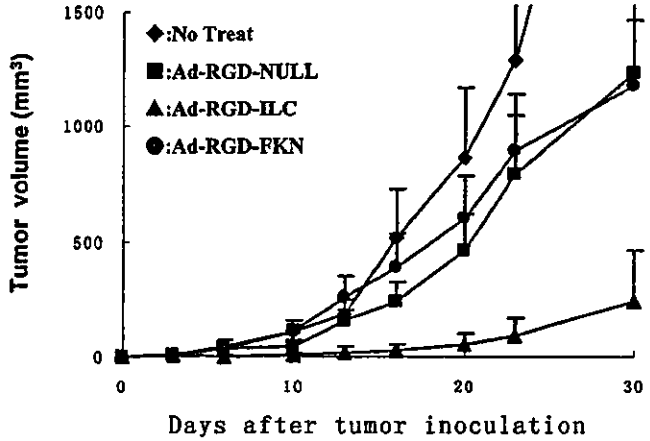

Fig. 3. Growth of OV-HM tumor cells, infected with chemokine-encoding adenovirus vectors, in B6C3F1 mice. Mice were inoculated intradermally in the flank with 1×10^6 OV-HM cells (100 μl in RPMI 1640) infected at an MOI of 10 with Ad-RGD-mILC or Ad-RGD-mFKN for 24 h. Tumor volume was calculated after measuring the length and width of the tumor at indicated periods of time, and data are expressed as the mean ± SE of results obtained from at least five mice. Animals were euthanized when one of the two values measured was >15 mm.

retarded growth of tumor (data not shown). In contrast, 100% of the mice rechallenged with B16/BL6 developed palpable tumors within 2 weeks. These results indicated the generation of specific immunity against OV-HM in mice that rejected OV-HM-expressing mILC. We also confirmed that OV-HM infected with Ad-RGD-mILC did not show such marked growth suppression in nude mice deficient in T cells (Fig. 4). These results suggested that the importance of T cells in the antitumor effect against OV-HM-expressing mILC.

Infiltration of T and NK Cells into Tumor Infection with Ad-RGD-mILC and Ad-RGD-mFKN. To examine the antitumor mechanism of Ad-RGD-mILC, tumor tissues were immunohistochemically stained for CD3 (a T-cell marker) and asialoGM1 (an NK-cell marker; Refs. 25 and 26) 2 days after the inoculation of OV-HM cells infected with Ad-RGD-mILC, Ad-RGD-mFKN, or Ad-RGD-NULL. As shown in Figs. 5 and 6, both OV-HM cells infected with Ad-RGD-mILC and Ad-RGD-mFKN demonstrated the accumulation of CD3$^+$ T and NK cells in tumor tissues. CD3$^+$ T and NK cells were evenly distributed in the tumor tissue of OV-HM infected with Ad-RGD-mILC. However, these cells were mostly accumulated around the tumor blood vessel in the tumor tissues of OV-HM infected with Ad-RGD-mFKN. Furthermore, promoted growth of tumor blood vessels appeared to be present in OV-HM-expressing mFKN (Figs. 5 and 6).

Involvement of CD4$^+$ and CD8$^+$ T Cells in the Antitumor Effect of mILC. To investigate the role of T and NK cells in the antitumor effect by Ad-RGD-mILC, B6C3F1 mice selectively depleted with CD4$^+$ T, CD8$^+$ T, or NK cell were inoculated with OV-HM cells infected with Ad-RGD-mILC. As shown in Fig. 7, no tumor grew in the NK cell-depleted group, whereas tumors efficiently developed in both of the CD4$^+$ or CD8$^+$ T cell-depleted mice. These results indicated that the inhibition of tumor growth by mILC was mostly dependent on CD4$^+$ and CD8$^+$ T cells but not on NK cells.

DISCUSSION

Cytokine or chemokine encoded by a viral vector is currently regarded as a promising way of cancer gene immunotherapy. Researchers have paid attention to chemotactic activity of chemokines for immune cells and expected that they may be able to play an important role in cancer treatment, because the basis and premise of immunotherapy is the accumulation of immune cells in tumor tissues.

The CC chemokine ILC, also called cutaneous T cell-attracting

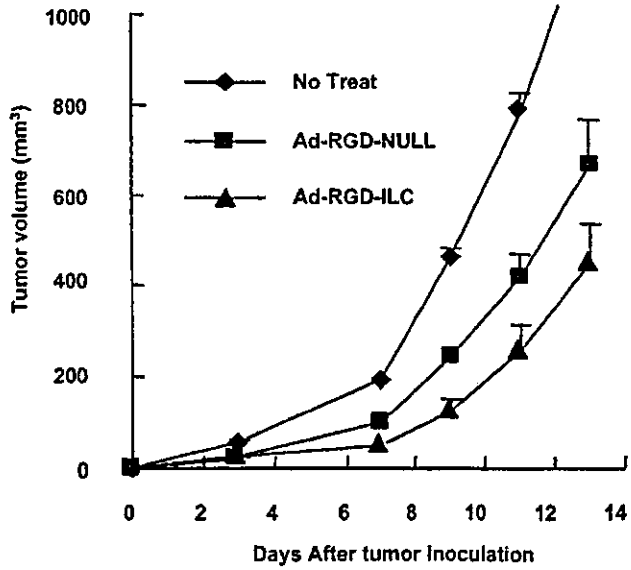

Fig. 4. Growth of OV-HM tumor cells infected with Ad-RGD-mILC in BALB/c nude mice. Mice were inoculated intradermally in the flank with 1×10^6 OV-HM cells (100 μl in RPMI 1640) infected at an MOI of 10 with Ad-RGD-mILC or Ad-RGD-mFKN for 24 h. Tumor volume was calculated after measuring the length and width of the tumor at indicated periods of time, and data are expressed as the mean ± SE of results from at least five mice.

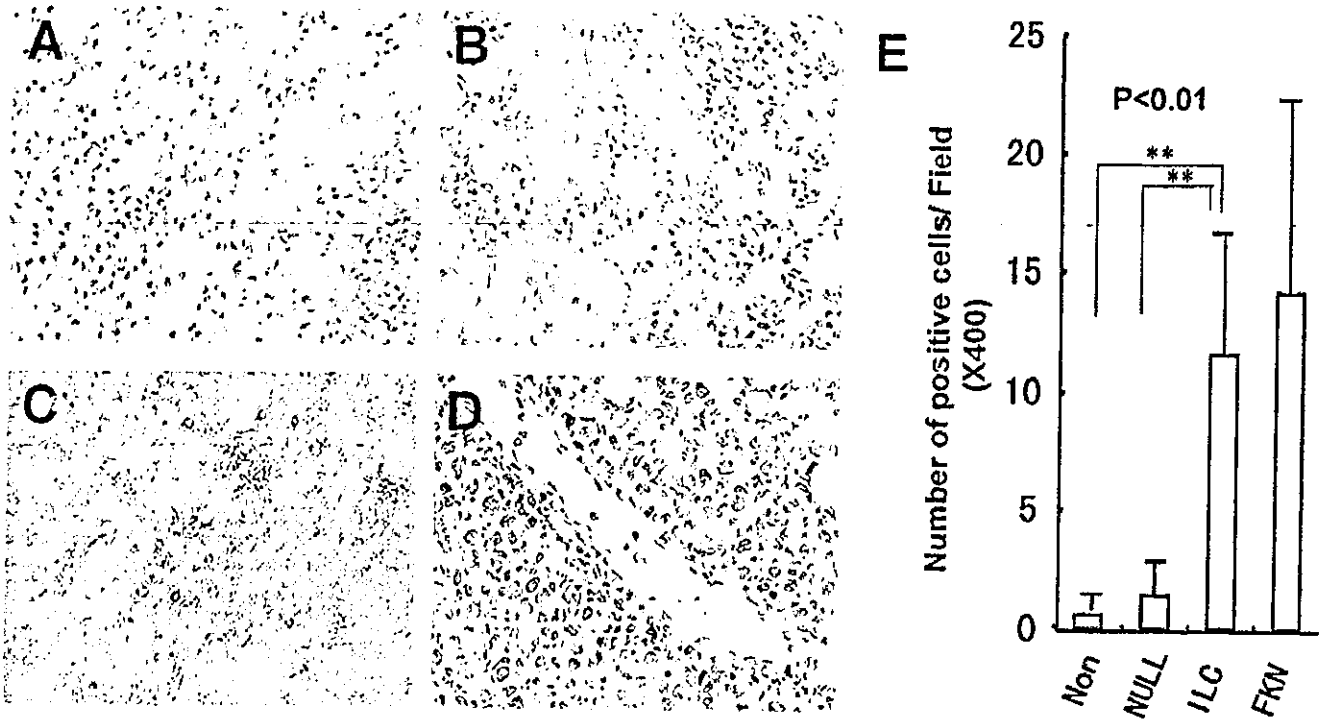

Fig. 5. CD3-positive lymphocytes infiltrate into OV-HM tumors infected with Ad-RGD-mILC and Ad-RGD-mFKN. *A–D*, representative immunohistochemical appearances of tumor nodules from mice inoculated intradermally with 1×10^6 OV-HM cells infected with none (*A*), Ad-RGD-NULL (*B*), Ad-RGD-mILC (*C*), or Ad-RGD-mFKN (*D*). Statistical analysis was carried out by Welch's *t* test.

chemokine or CCL27, was reported to recruit T cells to the site of its injection (27). The CX_3C family chemokine FKN (also called CX_3CL1) could also attract a variety of cytotoxic lymphocytes (13, 14, 28) and enhance the cytotoxicity of NK cells (29). In the present study, we hypothesized that the transfer of the mILC or mFKN gene to tumor cells, by using recombinant adenovirus *in vitro*, could render the tumor to express the chemokine *in vivo*. The chemokine would consequently induce the accumulation of immune cells in the tumor

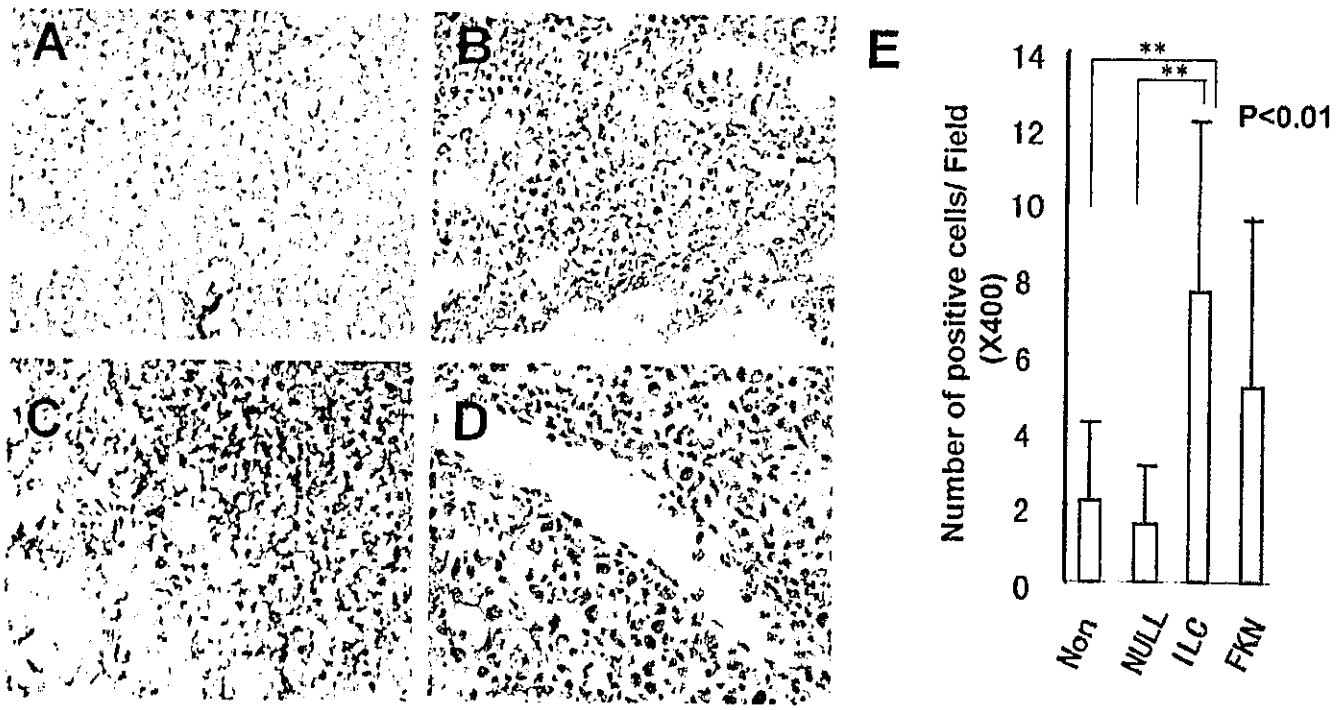

Fig. 6. NK cells infiltrate into OV-HM tumors infected with Ad-RGD-mILC and Ad-RGD-mFKN. *A–D*, representative immunohistochemical appearances of tumor nodules from mice inoculated intradermally with 1×10^6 OV-HM cells infected with none (*A*), Ad-RGD-NULL (*B*), Ad-RGD-mILC (*C*), or Ad-RGD-mFKN (*D*). Statistical analysis was carried out by Welch's *t* test.

Cancer Gene Therapy (2005) 12, 72–83

www.nature.com/cgt

Immunological properties and vaccine efficacy of murine dendritic cells simultaneously expressing melanoma-associated antigen and interleukin-12

Naoki Okada,[1] Sayaka Iiyama,[1] Yuka Okada,[2] Hiroyuki Mizuguchi,[3] Takao Hayakawa,[4] Shinsaku Nakagawa,[5] Tadanori Mayumi,[5] Takuya Fujita,[1] and Akira Yamamoto[1]

[1]Department of Biopharmaceutics, Kyoto Pharmaceutical University, 5 Nakauchi-cho, Misasagi, Yamashina-ku, Kyoto 607-8414, Japan; [2]Research Institute for Microbial Diseases, Osaka University, 3-1 Yamadaoka, Suita, Osaka 565-0871, Japan; [3]Division of Cellular and Gene Therapy Products, National Institute of Health Sciences, 1-18-1 Kamiyoga, Setagaya-ku, Tokyo 158-8501, Japan; [4]National Institute of Health Sciences, 1-18-1 Kamiyoga, Setagaya-ku, Tokyo 158-8501, Japan; and [5]Department of Biopharmaceutics, Graduate School of Pharmaceutical Sciences, Osaka University, 1-6 Yamadaoka, Suita, Osaka 565-0871, Japan.

Interleukin (IL)-12 is a key factor for inducing cellular immune responses, which play a central role in the eradication of cancer. In the present study, in order to create a dendritic cell (DC)-based vaccine capable of positively skewing immune response toward a cellular immunity-dominant state, we analyzed immunological characteristics and vaccine efficacy of DCs cotransduced with melanoma-associated antigen (gp100) and IL-12 gene (gp100 + IL12/DCs) by using RGD fiber-mutant adenovirus vector (AdRGD), which enables highly efficient gene transduction into DCs. gp100 + IL12/DCs could simultaneously express cytoplasmic gp100 and secretory IL-12 at levels comparable to DCs transduced with each gene alone. In comparison with DCs transduced with gp100 alone (gp100/DCs), upregulation of major histocompatibility complex class I, CD40, and CD86 molecules on the cell surface and more potent T-cell-stimulating ability for proliferation and interferon-γ secretion were observed as characteristic changes in gp100 + IL12/DCs. In addition, administration of gp100 + IL12/DCs, which were prepared by a relatively low dose of AdRGD-IL12, could induce more potent tumor-specific cellular immunity in the murine B16BL6 melanoma model than vaccination with gp100/DCs. However, antitumor effect and B16BL6-specific cytotoxic T-lymphocyte activity in mice vaccinated with gp100 + IL12/DCs diminished with increasing AdRGD-IL12 dose during gene transduction, and paralleled the decrease in presentation levels via MHC class I molecules for antigen transduced with another AdRGD. Collectively, our results suggested that optimization of combined vector dose was required for development of a more efficacious DC-based vaccine for cancer immunotherapy, which relied on genetic engineering to simultaneously express tumor-associated antigen and IL-12.
Cancer Gene Therapy (2005) **12,** 72–83. doi:10.1038/sj.cgt.7700772
Published online 24 September 2004

Keywords: dendritic cell; gene transduction; gp100; IL-12; melanoma

Dendritic cells (DCs) are potent professional antigen-presenting cells (APCs) that play a pivotal role in directing and amplifying the adaptive immune response to pathogens and infected/mutated cells.[1,2] The ability of DCs to stimulate naive T cells has long been thought to be crucial in initiating an effective immune response, and DCs are uniquely situated at the interface between the innate and adaptive immune systems. Because of these immunological properties, DCs are currently under intense scrutiny as potential adjuvants for vaccines in many clinical settings. Studies in healthy volunteers and patients with cancer have shown that tumor-associated antigen (TAA)-pulsed DCs can boost both $CD8^+$ and $CD4^+$ T-cell responses *in vivo*.[3–5]

Although these promising findings encourage the development of DC-based immunotherapy for cancer, the establishment of DC-manipulation capable of supplementing optimal vaccine function is required for the achievement of sufficient efficacy in current therapy. We previously established a highly efficient gene transduction technique into DCs by applying RGD fiber-mutant adenovirus vector (AdRGD),[6,7] and demonstrated that DCs transduced with TAA gene using AdRGD are effective vaccine carriers for induction of tumor-specific immune responses in mice.[8,9] These results suggested that the AdRGD system is very useful for DC-manipulation

Received April 28, 2004.
Address correspondence and reprint requests to: Dr Naoki Okada, PhD, Department of Biopharmaceutics, Kyoto Pharmaceutical University, 5 Nakauchi-cho, Misasagi, Yamashina-ku, Kyoto 607-8414, Japan. E-mail: okadan@mb.kyoto-phu.ac.jp

through transduction of genes encoding immunofunctional molecules as well as for antigen gene delivery into DCs.

The immune system is roughly classified into cellular immunity and humoral immunity, and optimal immune response is achieved by balanced activation of both systems. Cellular immune response, based on the activation of natural killer (NK) cells and TAA-specific cytotoxic T lymphocytes (CTLs), plays a more important role in elimination of tumor cells by tumor immunity than humoral immune response accompanied by antibody production from B cells.[10–13] Therefore, an approach that biases immune balance toward the cellular immune response would enhance the efficacy of DC-based immunotherapy for cancer. Interleukin (IL)-12 is a 70 kDa (p70) heterodimer protein in which the 40 kDa (p40) and 35 kDa (p35) subunits are connected by one S–S bond.[14,15] IL-12 plays a key role in the induction of cellular immune responses, such as enhancement of proliferation and cytotoxic activity in NK cells and CTLs,[16,17] production of interferon (IFN)-γ from activated cells,[17–19] and promotion of differentiation of helper T-type 1 (Th1) cells from Th0 cells.[17,20,21] IFN-γ is involved in IL-12-mediated tumor regression,[22] and IL-12 also exhibits an antiangiogenic effect that can account for some antitumor activity.[23] Thus, it was strongly predicted that DCs cotransduced with the TAA and IL-12 genes may be efficacious vaccine carriers that can drastically improve effectiveness of DC-based immunotherapy for cancer by positively biasing immune balance toward cellular immunity, the Th1-dominant state, by inducing IL-12 secretion as well as by sensitizing TAA-specific CTLs via TAA-peptide presentation on major histocompatibility complex (MHC) molecules.

In the present study, by using AdRGD, which is superior in gene transduction efficiency to DCs, we created a DC vaccine that simultaneously expressed gp100, a melanoma-associated antigen, and IL-12, and investigated its immunological characteristics and vaccine efficacy.

Materials and methods

Cell lines and mice

The helper cell line, 293 cells, was obtained from JCRB cell bank (Tokyo, Japan) and cultured in Dulbecco's modified Eagle's medium supplemented with 10% fetal bovine serum (FBS) and antibiotics. CD8-OVA 1.3 cells,[24] a specific T–T hybridoma against ovalbumin $(OVA)^+$ H-2K^b (kindly provided by Dr CV Harding; Department of Pathology, Case Western Reserve University, Cleveland, OH), were maintained in Dulbecco's modified Eagle's medium supplemented with 10% FBS, 50 μM 2-mercaptoethanol (2-ME), and antibiotics. Murine melanoma B16BL6 cells (H-2^b; JCRB cell bank) were grown in minimum essential medium supplemented with 7.5% FBS and antibiotics. EL4 cells, a T-lymphoma cell line of C57BL/6 origin, and YAC-1 cells, a lymphoma cell line highly sensitive to NK cells, were purchased from ATCC (Manassas, VA) and maintained in RPMI 1640 medium supplemented with 10% FBS, 50 μM 2-ME, and antibiotics. Female C57BL/6 mice (H-2^b) and female BALB/c mice (H-2^d), ages 7–8 weeks, were purchased from SLC Inc. (Hamamatsu, Japan). All mice were held under specific pathogen-free conditions and the experimental procedures were in accordance with the Osaka University guidelines for the welfare of animals in experimental neoplasia.

Vectors

Replication-deficient AdRGD was based on the adenovirus serotype 5 backbone with deletions of regions E1 and E3. The RGD sequence for αv-integrin-targeting was inserted into the HI loop of the fiber knob using a two-step method as previously described.[25] AdRGD-IL12,[26] AdRGD-gp100,[7] AdRGD-OVA,[8] and AdRGD-Luc[25] were previously constructed by an improved *in vitro* ligation method,[25,27,28] and encoded the murine IL-12 gene derived from mIL12 BIA/pBluescript II KS(-) (kindly provided by Dr H Yamamoto; Department of Immunology, Graduate School of Pharmaceutical Sciences, Osaka University, Suita, Japan), the human gp100 gene derived from pAx1-CA h-gp100 (kindly provided by Dr H Hamada; Department of Molecular Medicine, Sapporo Medical University, Sapporo, Japan), the OVA gene derived from pAc-neo-OVA (kindly provided by Dr MJ Bevan; Department of Immunology, Howard Hughes Medical Institute, University of Washington, Seattle, WA), and the luciferase gene derived from pGL3-Control (Promega, Madison, WI), respectively. All recombinant AdRGDs were propagated in 293 cells, purified by two rounds of cesium chloride gradient ultracentrifugation, dialyzed, and stored at −80°C. Titers of infective AdRGD particles were evaluated by the end point dilution method using 293 cells.

Generation and viral transduction of DCs

DCs were prepared according to the method of Lutz et al[29] with slight modification. Briefly, bone marrow cells flushed from the femurs and tibias of C57BL/6 mice were seeded at 0.5–1 $\times 10^7$ cells per sterile 100-mm bacterial grade culture dish in 10 ml of RPMI 1640 containing 10% FBS, 40 ng/ml recombinant murine granulocyte/macrophage colony-stimulating factor (GM-CSF; kindly provided by KIRIN Brewery Co., LTD, Tokyo, Japan), 50 μM 2-ME, and antibiotics. On day 3, another 10 ml of culture medium was added to the dish for medium replenishment. On day 6, 10 ml of the culture supernatant was collected and centrifuged at 1500 rpm for 5 minutes at room temperature, and the pellet was resuspended in 10 ml of fresh culture medium, and then returned to the original dish to conserve unattached cells. On day 8, nonadherent cells were harvested and used as immature DCs. DCs cultured for another 24 hours with media containing 1 μg/ml lipopolysaccharide (LPS; Nacalai Tesque, Inc., Kyoto, Japan) were used as phenotypically mature DCs (LPS/DCs). In transduction using AdRGDs,

DCs were suspended at a concentration of 5×10^6 cells/ml in FBS-free RPMI 1640 and placed in a 15-ml conical tube. Each AdRGD was added at various multiplicity of infections (MOIs), the suspension was mixed well, and the tube was incubated at 37°C for 2 hours with occasional gentle agitation. The cells were washed three times with phosphate-buffered saline (PBS) and resuspended in a suitable solution for subsequent experiments.

Reverse transcription-polymerase chain reaction (RT-PCR) analysis

Transduced DCs and mock DCs were cultured on 100-mm bacterial grade culture dishes in GM-CSF-free culture medium for 24 hours. Total RNA was isolated from these cells and LPS/DCs using Sepasol-RNA I Super (Nacalai Tesque, Inc.) according to the manufacturer's instructions. RT proceeded for 60 minutes at 42°C in a 50 μl reaction mixture containing 5 μg total RNA treated with DNase I, 10 μl 5 × RT buffer, 5 mM $MgCl_2$, 1 mM dNTP mix, 1 μM random primer (9-mer), 1 μM oligo$(dT)_{20}$, and 100 U ReverTra Ace (TOYOBO Co., LTD, Osaka, Japan). PCR amplification of the gp100, IL-12p35, IL-12p40, and β-actin transcripts was performed in 50 μl of a reaction mixture containing 1 μl of RT-material, 5 μl 10 × PCR buffer, 1.25 U *Taq* DNA polymerase (TOYOBO Co., LTD), 1.5 mM $MgCl_2$, 0.2 mM dNTP, and 0.4 μM primers. The sequences of the specific primers were as follows: human gp100: forward, 5′-tgg aac agg cag ctg tat cc-3′; reverse, 5′-cct aga act tgc cag tat tgg c-3′; murine IL-12p35: forward, 5′-tgt tta cca ctg gaa cta cac aag a-3′; reverse, 5′-aga gct tca ttt tca ctc tgt aag g-3′; murine IL-12p40: forward, 5′-ctc acc tgt gac acg cct ga-3′; reverse, 5′-cag gac act gaa tac ttc tc-3′; murine β-actin: forward, 5′-tgt gat ggt ggg aat ggg tca g-3′; reverse, 5′-ttt gat gtc acg cac gat ttc c-3′. After denaturation for 2 minutes at 95°C, 20 cycles of denaturation for 30 seconds at 95°C, annealing for 30 seconds at 48°C (for IL-12p40), 58°C (for IL-12p35), or 60°C (for gp100 and β-actin), and extension for 30 seconds at 72°C were repeated and followed by completion for 4 minutes at 72°C. The PCR product was electrophoresed on a 3% agarose gel, stained with ethidium bromide, and visualized under ultraviolet radiation. EZ Load (BIO-RAD, Tokyo, Japan) was used as a 100 bp-molecular ruler. The expected PCR product sizes were 362 bp (gp100), 334 bp (IL-12p35), 431 bp (IL-12p40), and 514 bp (β-actin).

Intracellular staining method for human gp100 protein in transduced DCs

Transduced DCs were cultured on 100-mm bacterial grade culture dishes in GM-CSF-free culture medium for 24 hours. Cells (1×10^6) were fixed by incubation for 10 minutes in 2% paraformaldehyde, and then cell membranes were permeabilized by incubation for 5 minutes in 1% saponin. The cells were incubated with 100 μl staining buffer (PBS containing 0.1% bovine serum albumin and 0.01% NaN_3) containing the anti-FcγRII/III monoclonal antibody (mAb), 2.4G2 (rat $IgG_{2b,\kappa}$; BD Biosciences, San Jose, CA), to block nonspecific binding of the subsequently used mAbs. After 30 minutes, the cells were incubated for 60 minutes with 100 μl staining buffer containing the HMB50 mAb against human gp100 (mouse IgG_{2a}; Neomarkers, Fremont, CA), and then resuspended in 100 μl staining buffer containing fluorescein isothiocyanate-conjugated anti-mouse Ig_κ (187.1; BD Biosciences). After incubation for 30 minutes, 30,000 events of the stained cells were analyzed for human gp100 protein expression by a FACScalibur flow cytometer using CellQuest software (BD Biosciences). Between all incubation steps, cells were washed three times with staining buffer.

Evaluation of IL-12 secretion level in transduced DCs

Transduced DCs, LPS/DCs, and mock DCs were cultured on 24-well plates at 5×10^5 cells/500 μl in GM-CSF-free culture medium for 24 hours. The supernatants were collected and the IL-12 level was measured using a murine IL-12p40 ELISA KIT and a murine IL-12p70 ELISA KIT (Endogen, Rockford, IL).

Analysis of surface marker-expression

All immunoreagents used in this experiment were purchased from BD Biosciences. Transduced DCs, LPS/DCs, and mock DCs were cultured on 100-mm bacterial grade culture dishes in GM-CSF-free culture medium for 24 hours. Cells (1×10^6) in 100 μl staining buffer were incubated for 30 minutes on ice with the 2.4G2 mAb. Then, cells were resuspended in 100 μl staining buffer and incubated for 30 minutes on ice using the manufacturer's recommended amounts of biotinylated mAbs: 28-8-6 (anti-H-$2K^b/D^b$), AF6-120.1 (anti-I-A^b), 3/23 (anti-CD40), 16-10A1 (anti-CD80), and GL1 (anti-CD86). The cells were then resuspended in 100 μl staining buffer containing phycoerythrin-conjugated streptavidin at a 1:200 dilution, and nonspecific binding was measured using phycoerythrin-conjugated streptavidin alone. After incubation for 30 minutes on ice, 30,000 events of the stained cells were analyzed for surface phenotype by flow cytometry. Between all incubation steps, cells were washed three times with staining buffer.

Antigen-presentation assay

C57BL/6 DCs were transduced with various combinations of AdRGD-OVA, AdRGD-IL12, and AdRGD-Luc, and then seeded on a 96-well flat-bottom culture plate at a density of 1×10^5 cells/well. These cells were cocultured with 1×10^5 cells/well CD8-OVA 1.3 cells at 37°C for 20 hours. The response of stimulated CD8-OVA 1.3 cells was assessed by determining the amount of IL-2 released into an aliquot of culture medium (100 μl) using a murine IL-2 ELISA KIT (Amersham Biosciences, Piscataway, NJ).

Mixed leukocyte reaction (MLR)

Three kinds of T cells, including allogeneic naive T cells from intact BALB/c mice, syngeneic naive T cells from intact C57BL/6 mice, and syngeneic gp100-primed T cells

from C57BL/6 mice immunized intradermally with 1×10^6 DCs transduced with AdRGD-gp100 at 25 MOI 1 week earlier, were purified from the splenocytes of each mouse as nylon wool nonadherent cells, and were used as responder cells at 1×10^5 cells/well in 96-well plates. Transduced DCs, LPS/DCs, or mock DCs (stimulator cells) were inactivated by 50 μg/ml mitomycin C (MMC) for 30 minutes and added to responder cells in varying cell numbers. Cells were cocultured in 100 μl RPMI 1640 supplemented with 10% FBS, 50 μM 2-ME, and antibiotics at 37°C and 5% CO_2 for 3 days. Control wells contained either stimulator cells alone or responder cells alone. Cell cultures were pulsed with 5-bromo-2'-deoxyuridine (BrdU) during the last 18 hours, and then proliferation of responder cells was evaluated by Cell Proliferation ELISA, BrdU (Roche Diagnostics Co., Indianapolis, IN).

Analysis of Th1/Th2 cytokine secretion from syngeneic T cells stimulated by transduced DCs

C57BL/6 naive T cells were purified from splenocytes as nylon wool nonadherent cells, and were used as responder cells at 5×10^6 cells/well in 24-well plates. Transduced DCs (stimulator cells) were added to responder cells at 5×10^5 cells/well. Cells were cocultured in 1 ml RPMI 1640 supplemented with 10% FBS, 50 μM 2-ME, 10 U/ml recombinant murine IL-2 (PeproTech EC LTD, London, England) and antibiotics at 37°C and 5% CO_2 for 5 days. The supernatants were collected and the IFN-γ, IL-4, and IL-10 levels were measured using a murine IFN-γ ELISA KIT, a murine IL-4 ELISA KIT, and a murine IL-10 ELISA KIT (Biosource International, Camarillo, CA), respectively.

Tumor protection assay

Transduced DCs were intradermally injected into the left flank of C57BL/6 mice at 2×10^5 cells/50 μl. At 1 week after the vaccination, 2×10^5 B16BL6 melanoma cells were intradermally inoculated into the right flank of the mice. The major and minor axes of the tumor were measured using microcalipers, and the tumor volume was calculated by the following formula: (tumor volume; mm^3) = (major axis; mm) × (minor axis; mm)^2 × 0.5236. The mice were euthanized when one of the two measurements was greater than 20 mm.

Europium (Eu)-release assay for cytolytic activity of NK cells and CTLs

Transduced or mock DCs were administered once intradermally into C57BL/6 mice at 2×10^5 cells/50 μl. At 1 week after immunization, nonadherent splenocytes were prepared from these mice and directly used as NK effector cells. The splenocytes were restimulated *in vitro* using B16BL6 cells, which were cultured in media containing 100 U/ml recombinant murine IFN-γ (PeproTech EC LTD) for 24 hours and inactivated with 50 μg/ml MMC at 37°C for 30 minutes, at an effector:stimulator ratio of 10:1 in RPMI 1640 supplemented with 10% FBS, 50 μM 2-ME, and antibiotics. After 5 days, the splenocytes were collected and used as CTL effector cells. Target cells (YAC-1 and EL4 cells for NK assay; IFN-γ-stimulated B16BL6 and IFN-γ-stimulated EL4 cells for CTL assay) were Eu-labeled and an Eu-release assay was performed as previously described.[30] Cytolytic activity was determined using the following formula: (% of lysis) = [(experimental Eu-release − spontaneous Eu-release)/(maximum Eu-release − spontaneous Eu-release)] × 100. Spontaneous Eu-release of the target cells was <10% of maximum Eu-release by detergent in all assays.

Results

Gene expression in DCs cotransduced with gp100 and IL-12

We examined the cytopathic effects of AdRGD-IL12 and AdRGD-gp100 on gene transduction into DCs by using the Cell Counting Kit-8 (DOJINDO LABORATORIES, Kumamoto, Japan). At 48 hours posttransduction, viability of DCs transduced with AdRGD-IL12 alone or AdRGD-IL12 plus AdRGD-gp100 remained more than 90% at a vector dose of 200 MOI or less (data not shown). Expression levels of human gp100 and murine IL-12 subunit mRNAs in various transduced DCs were analyzed by RT-PCR at 24 hours after gene transduction (Fig 1). Human gp100-specific PCR products were detected at the same level only in DCs that were transduced with AdRGD-gp100 alone at 25 MOI (lane 1) or the combination of AdRGD-gp100 at 25 MOI and AdRGD-IL12 at various MOI (lanes 3, 4, and 5). PCR

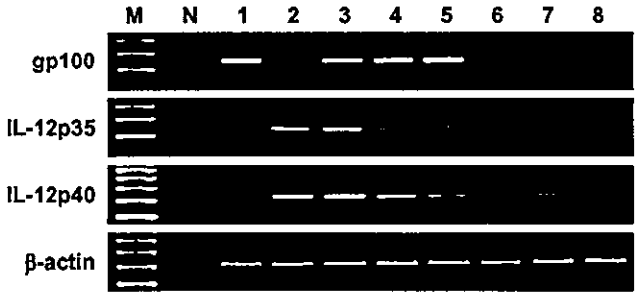

Figure 1 RT-PCR analysis of gp100, IL-12p35, and IL-12p40 in DCs cotransduced with AdRGD-gp100 and AdRGD-IL12. Total RNA was prepared from transduced, LPS-stimulated, or mock DCs, and then RT-PCR was performed as described in the Materials and methods section. The PCR products were electrophoresed through a 3% agarose gel, stained with ethidium bromide, and visualized under ultraviolet light. Lane M; 100 bp-molecular ruler, lane N; H_2O as template, lane 1; DCs transduced with AdRGD-gp100 alone at 25 MOI, lane 2; DCs transduced with AdRGD-IL12 alone at 25 MOI, lane 3; DCs cotransduced with AdRGD-gp100 at 25 MOI and AdRGD-IL12 at 25 MOI, lane 4; DCs cotransduced with AdRGD-gp100 at 25 MOI and AdRGD-IL12 at 12.5 MOI, lane 5; DCs cotransduced with AdRGD-gp100 at 25 MOI and AdRGD-IL12 at 5 MOI, lane 6; DCs transduced with AdRGD-Luc alone at 25 MOI, lane 7; LPS-stimulated (mature) DCs, lane 8; mock (immature) DCs.

products of IL-12p35 and IL-12p40 mRNA increased in an MOI-dependent manner for AdRGD-IL12 in DCs cotransduced with AdRGD-gp100 and AdRGD-IL12 (lanes 3, 4, and 5), and their levels were equal in DCs transduced with AdRGD-IL12 alone at 25 MOI (lane 2) and DCs cotransduced with AdRGD-gp100 at 25 MOI and AdRGD-IL12 at 25 MOI (lane 3). In addition, DCs transduced with AdRGD-gp100 alone (lane 1) or AdRGD-Luc (control vector) alone (lane 6) exhibited slightly higher IL-12p40 mRNA expression than mock DCs (lane 8), and IL-12p40 mRNA levels of LPS/DCs (lane 7) were comparable with those of DCs cotransduced with AdRGD-gp100 at 25 MOI and AdRGD-IL12 at 5 MOI (lane 5).

In order to confirm cytoplasmic expression of human gp100 protein, we performed flow cytometric analysis by the intracellular staining method using HMB50 mAb (Fig 2a). Under transductional conditions using AdRGD-gp100 at 25 MOI, about 70% of DCs could express gp100 protein in their cytoplasm whether or not the DCs were cotransduced individually with AdRGD-IL12 or AdRGD-Luc at 25 MOI. Gene expression intensity (mean fluorescence intensity; MFI) of gp100 in cotransduced DCs was also comparable to that of DCs transduced with AdRGD-gp100 alone. These data clearly demonstrated that the expression level of endogenous antigen transduced with AdRGD was not affected by cotransduction of AdRGD-IL12 in DCs. Likewise, IL-12 secretion levels in DCs transduced with various combinations of AdRGD-gp100 and AdRGD-IL12 were investigated by ELISA (Fig 2b). MOI-dependent IL-12p70, the biologically active form, and IL12p40 secretion into culture media of DCs cotransduced with AdRGD-gp100 and AdRGD-IL12 was detected at levels equivalent to those of DCs transduced with AdRGD-IL12 alone. Although LPS/DCs could secrete a large quantity of IL-12p40 into culture media, secretion of the active form, IL-12p70, was maintained at low levels, reflecting the low levels of IL-12p35 mRNA expression in RT-PCR analysis.

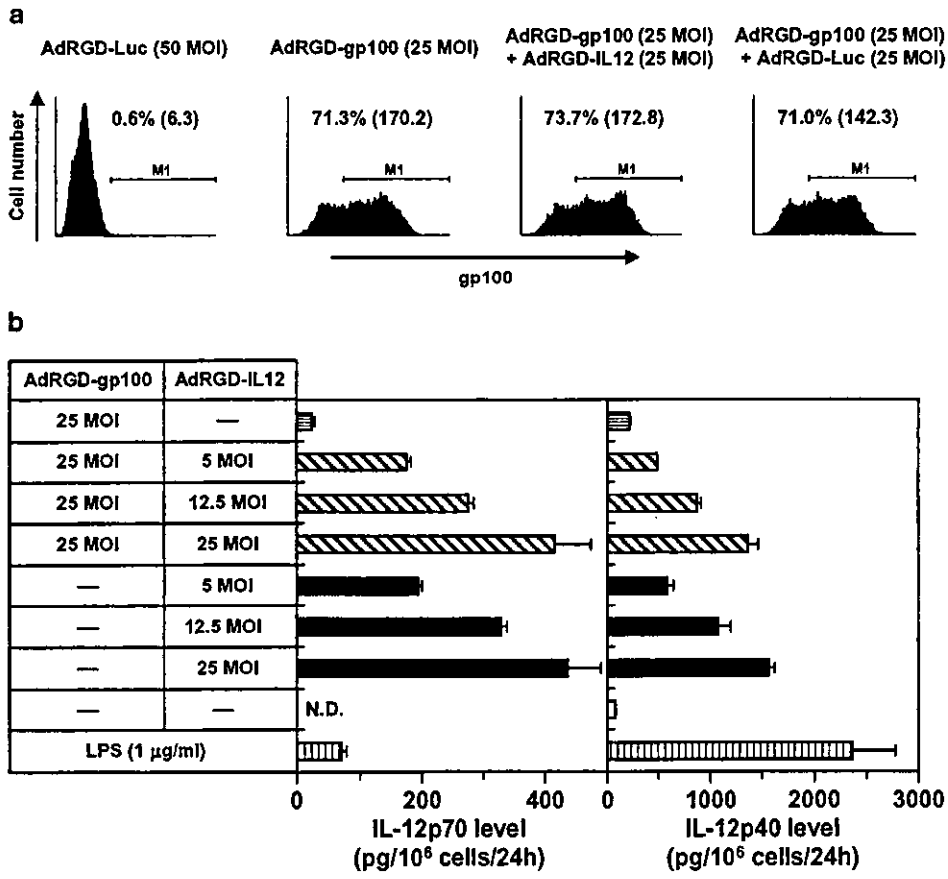

Figure 2 gp100 and IL-12 expression in DCs cotransduced with AdRGD-gp100 and AdRGD-IL12. (a) DCs were transduced with the indicated combinations of various AdRGDs at the indicated MOI for 2 hours. At 24 hours posttransduction, human gp100 gene expression was assessed by flow cytometric analysis. The percentage value and the numerical value in the parenthesis express percentage of M1-gated cells and mean fluorescence intensity (MFI), respectively. The data are representative of two independent experiments. (b) DCs were cotransduced with AdRGD-IL12 and AdRGD-gp100 at the indicated MOI for 2 hours. DCs treated with 1 μg/ml LPS for 24 hours were used as positive controls for phenotypical DC-maturation. After 24 hours cultivation, concentration of murine IL-12p70 and IL-12p40 in culture supernatants was measured by ELISA. The data are presented as mean±SD of three independent cultures. ND: IL-12p70 secreted from DCs was not detectable.

Immunological characteristics of DCs cotransduced with gp100 and IL-12

We first analyzed the expression levels of MHC/costimulatory molecules by flow cytometry in DCs prepared with various combinations of AdRGD-gp100 and AdRGD-IL12 (Fig 3). In comparison with mock DCs, DCs transduced with AdRGD-gp100 alone exhibited upregulated expression of all tested surface marker molecules, which play critical roles in the sensitization/activation of T cells, as was seen in mature LPS/DCs. This result agreed with our previous report demonstrating that transduction using AdRGD, irrespective of the type of inserted transgene, could enhance the expression of MHC/costimulatory molecules on DCs.[7] In addition, enhanced expression of MHC class I, CD40 and CD86 was observed as a characteristic change in DCs cotransduced with AdRGD-gp100 and AdRGD-IL12 as well as DCs transduced with AdRGD-IL12 alone. As upregulation of these molecules was dependent on MOI of combined AdRGD-IL12, the results suggested that the secreted IL-12 promoted maturation of DCs by an autocrine mechanism.

Next, we compared antigen presentation levels via MHC class I molecules by bioassay using T–T hybridoma, CD8-OVA 1.3 cells, between DCs transduced with various combinations of AdRGD-OVA, AdRGD-IL12, and AdRGD-Luc (Fig 4). In comparison with DCs transduced with AdRGD-OVA alone, DCs cotransduced with AdRGD-OVA and AdRGD-IL12 showed a slight decrease in IL-2 released from CD8-OVA 1.3 cells by vector dose-increase of combined AdRGD-IL12. The OVA-presentation levels in AdRGD-OVA-transduced DCs were not affected by the addition of exogenous recombinant murine IL-12 into culture media during the antigen-presentation assay (data not shown). In addition, an obvious decline in the OVA-presentation level was observed in DCs cotransduced with AdRGD-OVA and AdRGD-Luc, suggesting that competition may occur during a particular step of the MHC class I

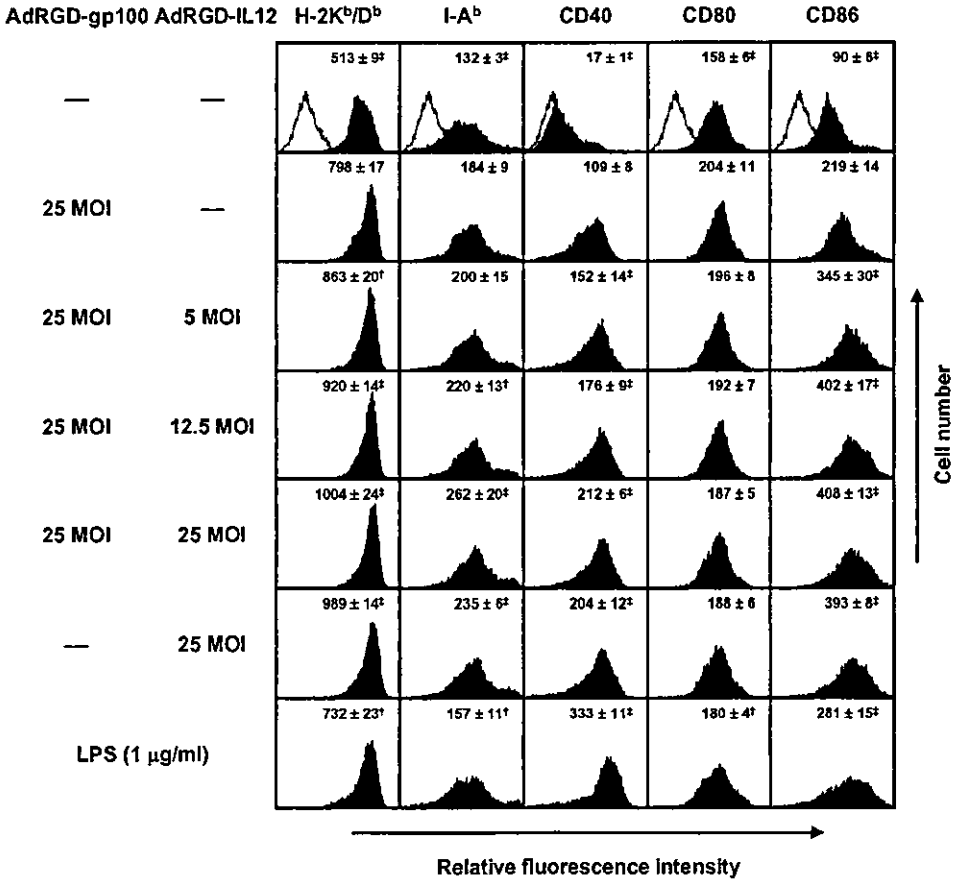

Figure 3 Flow cytometric analysis of surface markers in DCs cotransduced with gp100 and IL-12 gene by AdRGD. DCs were cotransduced with AdRGD-gp100 and AdRGD-IL12 at the indicated MOI for 2 hours. DCs treated with 1 μg/ml LPS for 24 hours were used as positive controls for phenotypical DC maturation. At 24 hours after transduction, cells were stained by indirect immunofluorescence using biotinylated mAbs of the indicated specificities (solid histogram). Dotted histograms represent cells stained by phycoerythrin-conjugated streptavidin alone. The data are representative of three independent experiments, and values indicated in the upper part of each panel represent MFI (mean ± SD) of flow cytometric analysis. The statistical analysis was carried out by Student's *t*-test. †$P<.05$, ‡$P<.01$ *versus* DCs transduced with AdRGD-gp100 alone at 25 MOI.

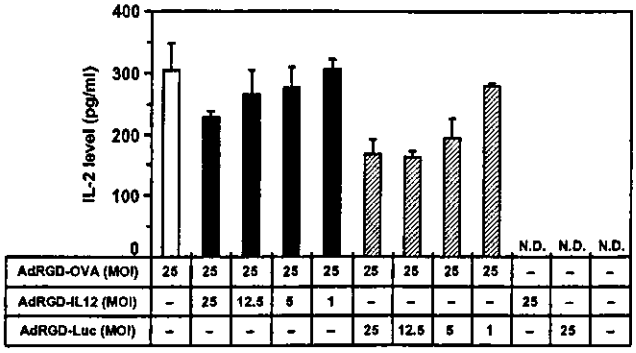

AdRGD-OVA (MOI)	25	25	25	25	25	25	25	25	25	–	–	–
AdRGD-IL12 (MOI)	–	25	12.5	5	1	–	–	–	–	25	–	–
AdRGD-Luc (MOI)	–	–	–	–	–	25	12.5	5	1	–	25	–

Figure 4 Antigen presentation on MHC class I molecules by DCs cotransduced with OVA and IL-12 gene by AdRGD. DCs were cotransduced with AdRGD-OVA and either AdRGD-IL12 or AdRGD-Luc at the indicated MOI for 2 hours. The levels of OVA peptide presentation via MHC class I molecules by transduced DCs were determined by bioassay using CD8-OVA 1.3 cells. The data represent the mean ± SD of three independent cultures. ND: IL-2 secreted from CD8-OVA 1.3 cells was not detectable.

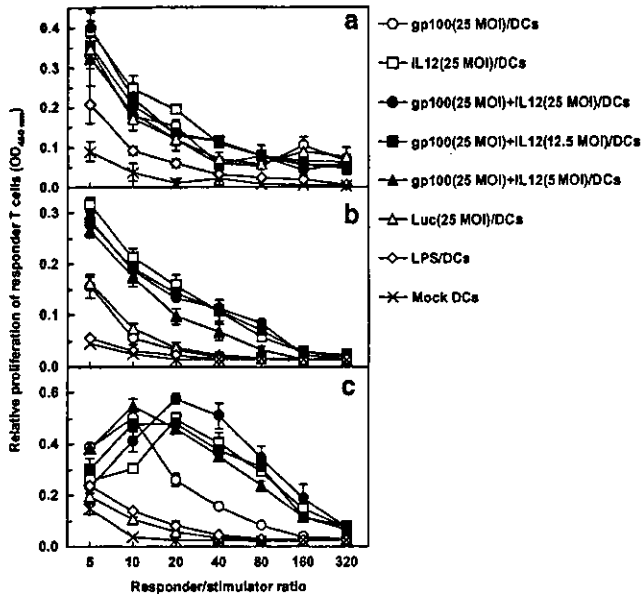

Figure 5 Allogeneic and syngeneic T-cell proliferation-stimulating ability of DCs cotransduced with gp100 and IL-12 gene by AdRGD. C57BL/6 DCs were transduced with the indicated combinations of various AdRGDs at the indicated MOI for 2 hours. Naive BALB/c T lymphocytes (**a**), naive C57BL/6 T lymphocytes (**b**), or gp100-primed C57BL/6 T lymphocytes (**c**), were cocultured with transduced, LPS-stimulated, or mock DCs at different responder/stimulator ratios for 3 days. Cell cultures were pulsed with BrdU during the last 18 hours, and then T-cell proliferation was assessed by BrdU-ELISA. Results are expressed as mean ± SE of three independent cultures using T cells prepared from three individual mice.

antigen-presentation pathway in DCs simultaneously expressing distinct proteins due to the presence of multiple AdRGDs. The variation in effects of coexpressed endogenous antigens in DCs might be induced by proteins accumulating in the cytoplasm and secreted to extracellular fluid, such as luciferase and IL-12, respectively. Taken together, antigen-presenting levels via MHC class I molecules on DCs transduced with AdRGD encoding antigen were slightly decreased by increasing dose of combined AdRGD-IL12.

T-cell-stimulating ability of DCs cotransduced with gp100 and IL-12

We performed allogeneic and syngeneic MLR to compare T-cell proliferation-stimulating ability of DCs transduced with AdRGD-gp100 alone or a combination of AdRGD-gp100 and AdRGD-IL12. DCs transduced with AdRGD-gp100 alone at 25 MOI (gp100(25MOI)/DCs), AdRGD-IL12 alone at 25 MOI (IL12(25MOI)/DCs), AdRGD-Luc alone at 25 MOI (Luc(25MOI)/DCs), or various combinations of AdRGD-gp100 and AdRGD-IL12 (gp100 (25MOI) + IL12(25MOI)/DCs, gp100(25MOI) + IL12(12.5 MOI)/DCs, and gp100(25MOI) + IL12(5MOI)/DCs) could equally stimulate proliferation of allogeneic naive T cells used as responder cells (Fig 5a). In addition, T-cell proliferation levels in these groups were higher than those not only in mock DCs but also LPS/DCs. These data indicated that DCs transduced by using AdRGD could sufficiently provide proliferative stimuli to T cells through allogeneic interaction of MHC molecules/T-cell receptors and costimulatory signals, regardless of the quantity of IL-12 secreted from DCs. On the other hand, IL12(25-MOI)/DCs, gp100(25MOI) + IL12(25MOI)/DCs, gp100 (25MOI) + IL12(12.5MOI)/DCs, and gp100(25MOI) + IL12(5MOI)/DCs could more strongly stimulate syngeneic naive T-cell proliferation as compared with gp100(25MOI)/DCs or Luc(25MOI)/DCs (Fig 5b), suggesting that *in vitro* syngeneic naive T-cell proliferation by DCs cotransduced with AdRGD-gp100 and AdRGD-IL12 was greatly influenced by secreted IL-12 rather than antigen-presentation via MHC molecules. Furthermore, in comparison with gp100(25MOI)/DCs, DCs transduced with AdRGD-IL12 alone or in combination with AdRGD-gp100 could induce considerable proliferation of syngeneic gp100-primed T cells, which were purified from C57BL/6 mice vaccinated beforehand with 10^6 gp100(25MOI)/DCs (Fig 5c). However, proliferation levels of syngeneic gp100-primed T cells stimulated by DCs transduced with AdRGD-IL12 alone or in combination with AdRGD-gp100 decreased at high responder/stimulator ratios, and this suppressive effect became remarkable at high AdRGD-IL12 MOI during gene transduction. These observations suggested that excessive IL-12 secreted from transduced DCs might inhibit proliferation or induce cell death in activated T cells.

In addition, we assessed by ELISA the Th1/Th2 cytokine balance in media of syngeneic naive T cells cocultured with various transduced DCs for 5 days at a responder/stimulator ratio of 10 in the presence of 10 U/ml recombinant murine IL-2 (Table 1). IL12(25MOI)/DCs, gp100(25MOI) + IL12(25MOI)/DCs, gp100(25MOI) + IL12(12.5MOI)/DCs, and gp100(25MOI) + IL12(5MOI)/DCs could markedly enhance Th1-skewing IFN-γ secretion from syngeneic naive T cells as compared with mock

Table 1 Cytokine secretion from syngeneic naive T cells cocultured with various transduced DCs

DC treatment				
AdRGD-gp100 (MOI)	AdRGD-IL12 (MOI)	IFN-γ (ng/ml)	IL-4 (pg/ml)	IL-10 (pg/ml)
—	—	0.25±0.05	<15	<30
25	—	1.00±0.19	<15	<30
—	25	17.17±0.48	<15	<30
25	25	25.78±1.84	<15	<30
25	12.5	18.61±1.47	<15	<30
25	5	20.23±2.96	<15	<30

Data are expressed as mean±SD of three independent cultures.

DCs, whereas only a slight increase in IFN-γ levels was observed during cocultivation with gp100(25MOI)/DCs. We confirmed that IFN-γ secretion was undetectable in control wells in which only transduced or mock DCs were cultured. On the other hand, secretion of the Th2 cytokines, IL-4 and IL-10, was not detectable in any syngeneic T cells stimulated by transduced or mock DCs. These results suggested that DCs cotransduced with gp100 and IL-12 could more efficiently differentiate sensitized T cells at the Th1-biasing state (the cellular immunity-dominant state), which is required for the induction of efficacious tumor immunity.

Vaccine efficacy of DCs cotransduced with gp100 and IL-12

In order to evaluate the potency of DCs cotransduced with gp100 and IL-12 as vaccine carriers, we investigated protective efficacy against murine B16BL6 melanoma challenge (Fig 6). C57BL/6 mice received a single intradermal injection of 2×10^5 DCs transduced with various combinations of AdRGD-gp100, AdRGD-IL12, and AdRGD-Luc, and then these mice were inoculated with 2×10^5 B16BL6 melanoma cells at 1 week post-immunization. Obvious growth suppression of the challenging B16BL6 tumor was achieved in mice vaccinated with gp100(25MOI)/DCs, as shown in our previous report,[9] whereas the mice immunized with IL12(25-MOI)/DCs or Luc(25MOI)/DCs showed little or no protective effect as compared with vehicle-injected mice. In addition, a more potent inhibitory effect on tumor growth could be observed in mice after vaccination with gp100(25MOI)+IL12(5MOI)/DCs than in mice vaccinated with gp100(25MOI)/DCs. However, vaccine efficacy of DCs cotransduced with gp100 and IL-12 tended to diminish with increasing AdRGD-IL12 MOI during gene transduction, and immunization with gp100(25MOI)+Luc(25MOI)/DCs led to inferior anti-tumor effects compared to those of the gp100(25MOI)/DCs group.

Furthermore, we investigated the cytolytic activities of NK cells and CTLs in mice intradermally immunized with DCs cotransduced with gp100 and IL-12 by Eu-release

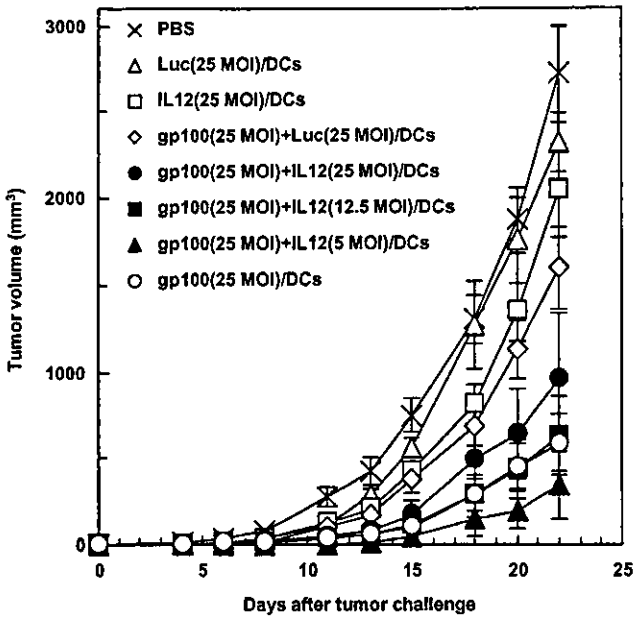

Figure 6 Vaccine efficacy of DCs cotransduced with gp100 and IL-12 gene by AdRGD against B16BL6 melanoma challenge. DCs were transduced with the indicated combinations of various AdRGDs at the indicated MOI for 2 hours. C57BL/6 mice were immunized by intradermal injection of transduced DCs into the left flank at 2×10^5 cells, and then 2×10^5 B16BL6 melanoma cells were inoculated into the right flank of the mice 1 week postvaccination. The size of tumors was assessed using microcalipers three times per week. Each point represents the mean±SE of 6–12 mice. Statistical analysis of tumor volume on day 22 after tumor challenge was carried out by Mann-Whitney *U*-test. $P<.01$ (■, ▲, ○), $P<.05$ (●), not significant (×, □, ◇) *versus* Luc(25MOI)/DCs (△). $P<.01$ (×, △, □, ◇), not significant (●, ■, ▲) *versus* gp100(25MOI)/DCs (○).

assay. At 1 week after immunization of C57BL/6 mice with various DC vaccines, the splenocytes were used in a cytolytic assay against YAC-1 and EL4 cells, and were restimulated *in vitro* with inactivated B16BL6 cells, which were treated with recombinant murine IFN-γ to promote the expression of their MHC class I molecules, for CTL expansion. As shown in Figure 7a, the splenic cytolytic activity against YAC-1 cells markedly increased after immunization with gp100(25MOI)+IL12(25MOI)/DCs as well as IL12(25MOI)/DCs, whereas EL4 cells were not injured by splenocytes prepared from any groups. Effector cells from mice immunized with gp100(25MOI)+IL12(5MOI)/DCs exhibited equivalent NK activity to those from mice immunized with gp100(25MOI)/DCs. These data indicated that the non-specific NK activity involved in the anti-B16BL6 melanoma response was enhanced with the increase in IL-12 secretion from the administered DC vaccine. On the other hand, the cytolytic effects on B16BL6 cells by *in vitro* restimulated effector cells was promoted in mice immunized with gp100(25MOI)+IL12(5MOI)/DCs as compared with mice immunized with gp100(25MOI)/DCs (Fig 7b). This cytolytic activity was caused by B16BL6-specific CTLs because the effector cells prepared from

mice immunized with IL12(25MOI)/DCs or mock DCs did not injure the B16BL6 cells and no cytolytic effects against syngeneic irrelevant EL4 cells were detected in any group. However, consistent with the protective effect against B16BL6 tumor challenge, mice vaccinated with gp100(25MOI) + IL12(25MOI)/DCs showed lower B16BL6-specific CTL activity than mice immunized with gp100(25MOI)/DCs.

Therefore, immunization with DCs genetically modified to express simultaneously gp100 and IL-12 exhibited duplicity for the host's immune response in our experimental model. That is, as compared with DCs transduced with AdRGD-gp100 alone, DCs cotransduced with AdRGD-IL12 at a relatively low ratio to AdRGD-gp100 were equal in inducibility of NK activity, but could more efficiently induce anti-B16BL6 tumor effects and antigen-specific CTL activity. In contrast, DCs combined with a high dose of AdRGD-IL12 during gene transduction could enhance NK activity, but attenuated B16BL6-protective efficacy and CTL activity.

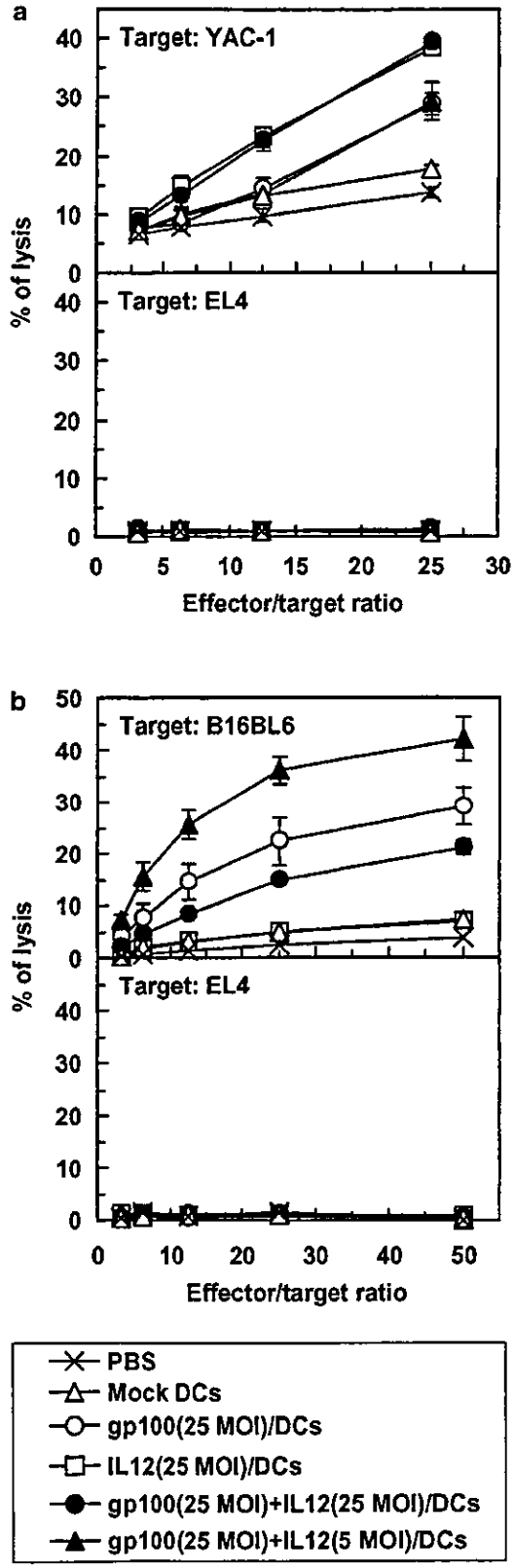

Discussion

Since DCs are the most potent APCs and are uniquely capable of presenting novel antigens to naive T cells to initiate and modulate immune responses,[1,2] various DC-based vaccines for use in immune intervention strategies against cancer have been designed and studied in many research organizations. Antitumor CTLs play a central role in the tumor-specific immune response, and the efficient priming and subsequent activation of antitumor CTLs requires the processing and presentation of TAAs as peptide fragments in the context of appropriate MHC class I molecules by APCs.[31] In addition, a Th1-biased cytokine balance is desirable for sensitization of CTLs specific for TAA by APCs. IL-12 is the key factor that skews the immune balance toward a Th1 response and that can promote a switch from an established Th2 to a Th1 response.[32,33] In fact, potent antitumor effects of DCs genetically engineered with IL-12 have been demonstrated in several murine models by vaccination using TAA-derived peptide pulsed DCs or intratumoral injection using unpulsed DCs.[34–36] Therefore, we believe that, as compared with DCs delivered with TAA gene alone, DCs genetically manipulated to express simultaneously TAA and IL-12 might be a promising vaccine carrier

Figure 7 NK (a) and B16BL6-specific CTL (b) activity in mice immunized with DCs cotransduced with gp100 and IL-12 gene by AdRGD. DCs were transduced with the indicated combinations of AdRGD-gp100 and AdRGD-IL12 at the indicated MOI for 2 hours. Transduced or mock DCs were vaccinated once intradermally into C57BL/6 mice at 2×10^5 cells. At 1 week after immunization, nonadherent splenocytes were prepared from these mice, and directly used in cytolytic assays against YAC-1 and EL-4 cells (a). In addition, the isolated splenocytes were restimulated *in vitro* for 5 days with IFN-γ-stimulated and MMC-inactivated B16BL6 cells. A cytolytic assay using the restimulated splenocytes was performed against IFN-γ-stimulated B16BL6 and EL4 cells (b). Each point represents the mean ± SE of four independent cultures from four individual mice.

capable of generating more efficacious antitumor responses because of their ability to induce Th1-polarized responses.

A vector system, which can effectively deliver a foreign gene to DCs, is required to create a genetically modified DC vaccine having a potential to improve the efficacy of DC-based immunotherapy. We have demonstrated that AdRGD enabled highly efficient gene transduction into murine and human DCs because of the targeting of αv-integrin by the RGD sequence inserted at the HI-loop in their fiber knob.[6–9] When mouse bone marrow-derived DCs were cotransduced with AdRGD-gp100 and AdRGD-IL12, their expression of gp100 and IL-12 was comparable to that in DCs transduced with each AdRGD alone (Figs 1 and 2). IL-12 secreted from these DCs is biologically active because direct intratumoral injection of AdRGD-IL12, used in the present study and whose expression cassette was designed to be transcribed from IL-12p35 cDNA to the internal ribosome entry site sequence to IL-12p40 cDNA under the control of the cytomegalovirus promoter, could induce tumor regression based on promotion of tumor immunity in melanoma-bearing mice.[37] RT-PCR analysis (Fig 1) suggested that LPS-driven maturation or irrelevant AdRGD transduction could moderately enhance expression of the IL-12p40 subunit mRNA in DCs, but not IL-12p35 subunit mRNA. Several reports have demonstrated that the production of the two IL-12 subunits is regulated by different mechanisms, mainly at the level of mRNA expression, and that the level of bioactive IL-12p70 production in APCs in response to LPS and cytokines is determined by the level of IL-12p35 expression.[38,39] Therefore, DCs cannot attain sufficient IL-12p70 productivity, which is based on enhancement of endogenous gene expression of the two subunits, via a maturation signal from LPS or AdRGD transduction alone. Taken together, our results demonstrated that DCs cotransduced with AdRGD-gp100 and AdRGD-IL12 could simultaneously express gp100 and IL-12 at levels equal to DCs transduced with each vector alone, indicating that DCs can obtain several additional functions by using a combination of AdRGDs carrying different genes.

Full analysis and understanding of immunological characteristics of DC vaccine are imperative for the development of DC-based immunotherapy because the polarity of the immune response is greatly influenced by the activated state of DCs during T-cell sensitization. Flow cytometric analysis indicated that the expression of MHC class I/II, CD40, CD80, and CD86 molecules was enhanced only by AdRGD-transduction, and that DCs transduced with the IL-12 gene exhibited considerable upregulation of MHC class I, CD40, and CD86 molecules on their surface in response to autocrine effects of secreted IL-12 as compared with DCs transduced with AdRGD-gp100 alone (Fig 3). On the other hand, DCs cotransduced with OVA and IL-12 by AdRGDs exhibited lower OVA-presentation levels via MHC class I molecules than DCs transduced with AdRGD-OVA alone (Fig 4), although the cytoplasmic expression of endogenous antigen introduced into DCs was not affected by the combination with other AdRGDs (Fig 2a). In addition, OVA-presentation levels in DCs transduced with AdRGD-OVA were markedly decreased by combination with AdRGD-Luc, which expresses luciferase as another endogenous antigen (Fig 4). These inconsistent results suggested that processing machineries in the MHC class I-presentation pathway may compete with multiple proteins transduced by the combination of AdRGDs, and that localization characteristics, such as cytoplasmic accumulation, extracellular secretion, and plasma membrane-specific localization, of other proteins should be considered during the preparation of DCs expressing TAA and other functional proteins by cotransduction with multiple AdRGDs in an attempt to maintain sufficient TAA-presenting capacity. With regard to T-cell-stimulating ability, DCs cotransduced with gp100 and IL-12 could more effectively enhance proliferation of syngeneic naive and gp100-primed T cells than DCs transduced with gp100 alone, although allogeneic T-cell proliferation did not differ between the two types of transduced DCs (Fig 5). Furthermore, we could detect considerable IFN-γ secretion from syngeneic naive T cells stimulated by DCs cotransduced with gp100 and IL-12 (Table 1), as expected. These data from *in vitro* immunological analysis suggested that DCs cotransduced with TAA and IL-12 using AdRGD can function as useful vaccine carriers possessing TAA-presentation ability, sufficient T-cell-stimulating ability, and Th1-driving ability *in vivo*.

We attempted to compare vaccine efficacy of DCs genetically modified with various combinations of AdRGD-gp100, AdRGD-IL12, and AdRGD-Luc using the murine B16BL6 melanoma model. Although mice vaccinated with gp100(25MOI) + IL12(5MOI)/DCs exhibited more effective suppression of B16BL6 tumor growth and efficient induction of B16BL6-specific CTLs than those vaccinated with gp100(25MOI)/DCs, vaccine efficacy of cotransduced DCs diminished with increasing combined AdRGD-IL12 MOI during gene transduction, contrary to our expectation (Figs 6 and 7). We speculated that this adverse effect might be caused by a decrease in antigen presentation in DCs by coexpression of TAA and IL-12 as shown in Figure 4, because the anti-B16BL6 effect of gp100(25MOI) + Luc(25MOI)/DCs was obviously inferior to that by gp100(25MOI)/DCs. An alternative explanation for the negative effect of AdRGD-IL12-cotransduction includes an immunosuppressive effect of excess IL-12 on the host's immune cells. Several studies have demonstrated that IL-12 inhibits cell-mediated immune responses, such as clonal expansion of CTLs, in a dose-dependent manner through IFN-γ-mediated nitric oxide production by macrophages in the murine models.[40–43] The *in vivo* bimodal effect of DCs cotransduced with gp100 and IL-12 in our model might involve immunosuppression based on nitric oxide, because DCs transduced with AdRGD-IL12 could drastically enhance IFN-γ secretion from syngeneic naive T cells in MLR (Table 1). In addition, Piccioli et al[44] reported that an *in vitro* interaction between activated NK cells and DCs at high NK/DC ratios resulted in inhibition of DC functions due to potent killing by NK cells,

whereas this interaction at low NK/DC ratios led to drastic increases in DC cytokine production. Therefore, a remarkable increase in NK activity in mice that were vaccinated with gp100(25MOI) + IL12(25MOI)/DCs, as shown in Figure 7, might suppress the induction of the B16BL6-specific immune response by the administered DC vaccine.

To date, vaccine efficacy of DCs cotransduced with TAA and IL-12 has not been fully clarified because both positive[45] and negative[46] effects of simultaneous expression of IL-12 in DC vaccine have been reported. Based on the results of the present study, we concluded that determination of the specific vector dose capable of optimizing both TAA-presentation levels and IL-12-secretion levels in DC vaccine is essential for improving antitumor efficacy based on active biasing of the immune response toward a cellular immunity dominated state.

Abbreviations

2-ME, 2-mercaptoethanol; AdRGD, RGD fiber-mutant adenovirus vector; APC, antigen-presenting cell; BrdU, 5-bromo-2′-deoxyuridine; CTL, cytotoxic T lymphocyte; DC, dendritic cell; Eu, europium; FBS, fetal bovine serum; GM-CSF, granulocyte/macrophage colony-stimulating factor; IFN, interferon; IL, interleukin; LPS, lipopolysaccharide; mAb, monoclonal antibody; MHC, major histocompatibility complex; MLR, mixed leukocyte reaction; MMC, mitomycin C; MOI, multiplicity of infection; NK, natural killer; OVA, ovalbumin; PBS, phosphate-buffered saline; RT-PCR, reverse transcription-polymerase chain reaction; TAA, tumor-associated antigen; Th, helper T cell.

Acknowledgments

We are grateful to Dr Hiroshi Yamamoto (Department of Immunology, Graduate School of Pharmaceutical Sciences, Osaka University, Suita, Japan) for providing mIL12 BIA/pBluescript II KS(-), to Dr Hirofumi Hamada (Department of Molecular Medicine, Sapporo Medical University, Sapporo, Japan) for providing pAx1-CA h-gp100, to Dr Michael J Bevan (Department of Immunology, Howard Hughes Medical Institute, University of Washington, Seattle, WA) for providing pAc-neo-OVA, to Dr Clifford V Harding (Department of Pathology, Case Western Reserve University, Cleveland, OH) for providing CD8-OVA 1.3 cells, to Yasushige Masunaga, Masaya Nishida, and Aya Matsui (Department of Biopharmaceutics, Kyoto Pharmaceutical University, Kyoto, Japan) for technical assistance, and to KIRIN Brewery Co., Ltd (Tokyo, Japan) for providing recombinant murine GM-CSF.
The present study was supported in part by the Research on Health Sciences focusing on Drug Innovation from The Japan Health Sciences Foundation; by the Science Research Promotion Fund of the Japan Private School Promotion Foundation; by grants from the Bioventure Development Program of the Ministry of Education, Culture, Sports, Science and Technology of Japan; and by grants from the Ministry of Health, Labour and Welfare in Japan.

References

1. Banchereau J, Steinman RM. Dendritic cells and the control of immunity. *Nature*. 1998;392:245–252.
2. Kapsenberg ML. Dendritic-cell control of pathogen-driven T-cell polarization. *Nat Rev Immunol*. 2003;3:984–993.
3. Nestle FO, Alijagic S, Gilliet M, et al. Vaccination of melanoma patients with peptide- or tumor lysate-pulsed dendritic cells. *Nat Med*. 1998;4:328–332.
4. Thurner B, Haendle I, Roder C, et al. Vaccination with mage-3A1 peptide-pulsed mature, monocyte-derived dendritic cells expands specific cytotoxic T cells and induces regression of some metastases in advanced stage IV melanoma. *J Exp Med*. 1999;190:1669–1678.
5. Yu JS, Wheeler CJ, Zeltzer PM, et al. Vaccination of malignant glioma patients with peptide-pulsed dendritic cells elicits systemic cytotoxicity and intracranial T-cell infiltration. *Cancer Res*. 2001;61:842–847.
6. Okada N, Tsukada Y, Nakagawa S, et al. Efficient gene delivery into dendritic cells by fiber-mutant adenovirus vectors. *Biochem Biophys Res Commun*. 2001;282:173–179.
7. Okada N, Masunaga Y, Okada Y, et al. Gene transduction efficiency and maturation status in mouse bone marrow-derived dendritic cells infected with conventional or RGD fiber-mutant adenovirus vectors. *Cancer Gene Ther*. 2003;10:421–431.
8. Okada N, Saito T, Masunaga Y, et al. Efficient antigen gene transduction using Arg-Gly-Asp fiber-mutant adenovirus vectors can potentiate antitumor vaccine efficacy and maturation of murine dendritic cells. *Cancer Res*. 2001;61:7913–7919.
9. Okada N, Masunaga Y, Okada Y, et al. Dendritic cells transduced with gp100 gene by RGD fiber-mutant adenovirus vectors are highly efficacious in generating anti-B16BL6 melanoma immunity in mice. *Gene Therapy*. 2003;10:1891–1902.
10. Hammerling GJ, Klar D, Pulm W, et al. The influence of major histocompatibility complex class I antigens on tumor growth and metastasis. *Biochim Biophys Acta*. 1987; 907:245–259.
11. Moller P, Hammerling GJ. The role of surface HLA-A,B,C molecules in tumour immunity. *Cancer Surv*. 1992;13: 101–127.
12. Khanna R. Tumour surveillance: missing peptides and MHC molecules. *Immunol Cell Biol*. 1998;76:20–26.
13. Nishimura T, Nakui M, Sato M, et al. The critical role of Th1-dominant immunity in tumor immunology. *Cancer Chemother Pharmacol*. 2000;46(Suppl):S52–S61.
14. Gubler U, Chua AO, Schoenhaut DS, et al. Coexpression of two distinct genes is required to generate secreted bioactive cytotoxic lymphocyte maturation factor. *Proc Natl Acad Sci USA*. 1991;88:4143–4147.
15. Wolf SF, Temple PA, Kobayashi M, et al. Cloning of cDNA for natural killer cell stimulatory factor, a heterodimeric cytokine with multiple biologic effects on T and natural killer cells. *J Immunol*. 1991;146:3074–3081.
16. Robertson MJ, Soiffer RJ, Wolf SF, et al. Response of human natural killer (NK) cells to NK cell stimulatory